

A Thorough Comparison Between Independent Cascade and Susceptible-Infected-Recovered Models*

Panfeng Liu[†] Guoliang Qiu[†] Biaoshuai Tao[†] Kuan Yang[†]

Abstract

We study cascades in social networks with the independent cascade (IC) model and the Susceptible-Infected-recovered (SIR) model. The well-studied IC model fails to capture the feature of *node recovery*, and the SIR model is a variant of the IC model with the node recovery feature. In the SIR model, by computing the probability that a node successfully infects another before its recovery and viewing this probability as the corresponding IC parameter, the SIR model becomes an “out-going-edge-correlated” version of the IC model: the events of the infections along different out-going edges of a node become dependent in the SIR model, whereas these events are independent in the IC model. In this paper, we thoroughly compare the two models and examine the effect of this extra dependency in the SIR model. By a carefully designed coupling argument, we show that the seeds in the IC model have a stronger influence spread than their counterparts in the SIR model, and sometimes it can be significantly stronger. Specifically, we prove that, given the same network, the same seed sets, and the parameters of the two models being set based on the above-mentioned equivalence, the expected number of infected nodes at the end of the cascade for the IC model is weakly larger than that for the SIR model, and there are instances where this dominance is significant.

We also study the influence maximization problem (the optimization problem of selecting a set of nodes as initial seeds in a social network to maximize their influence) with the SIR model. We show that the above-mentioned difference in the two models yields different seed-selection strategies, which motivates the design of influence maximization algorithms specifically for the SIR model. We design efficient approximation algorithms with theoretical guarantees by adapting the reverse-reachable-set-based algorithms, commonly used for the IC model, to the SIR model.

1 Introduction

The study of information diffusion in social networks, such as Facebook, Twitter, and WeChat, has garnered significant attention in the fields of communication media and social science [Kempe et al., 2015, Domingos and Richardson, 2001, Brown and Reingen, 1987, Richardson and Domingos, 2002, Rigobon, 2002, Pastor-Satorras and Vespignani, 2001, Lerman and Ghosh, 2010]. Information diffusion is typically characterized by *cascading*—a fundamental social network process in which a number of nodes, called *seeds*, initially possess a certain attribute or piece of information and may spread to their neighbors.

Numerous diffusion models have been developed so far. Among them, the *independent cascade model* [Kempe et al., 2015] is well-known and extensively studied. In the independent cascade model (hereinafter denoted by IC), each edge (u, v) is assigned a probability $p_{u,v}$. An infected node u attempts to infect its neighbor v *only once*, with a success probability of $p_{u,v}$. The events of successful infections along different edges are independent. In the IC model, an infected node remains infected throughout the cascade.

However, in many real-world scenarios, an infected node may *recover*. This phenomenon can be observed in various situations. For example, consider when an individual subscribes to a magazine or signs up for a fitness membership card under the influence of friends; eventually, this subscription or membership may be terminated. This termination could result from factors such as the user losing interest in the service or the subscription/membership expiring. Another example arises when someone introduces a new product to a friend; initially, they may promote it, but eventually, they tire of advertising it after a few days. Similarly,

*A short version of this paper appears in AAAI’25.

[†]Shanghai Jiao Tong University {liupf22, guoliang.qiu, bstao, kuan.yang}@sjtu.edu.cn

when a user shares a post on Twitter, their friends may retweet it only for a short period before it becomes overshadowed by other posts. The recovery of nodes may signify the loss of a certain attribute or the end of spreading this attribute, both of which undoubtedly impact the cascading process.

The concept of node recovery is effectively captured by *epidemic models*. These models divide individuals into distinct states, including *susceptible*, *infected*, and *recovered*. Various models have been formulated based on feasible state transitions [Kermack and McKendrick, 1927, Allen, 1994, Greenwood and Gordillo, 2009]. The *Susceptible-Infected-Recovered model* [Kermack and McKendrick, 1927] (hereinafter denoted by SIR) includes the process from susceptible to infected and eventually to recovery and permanent immunity. In the SIR model, each node u has a *recover rate* γ_u . In each round, an infected node u attempts to infect each neighbor v , succeeding with probability $\beta_{u,v}$, and then the node u recovers with probability γ_u . If u does not recover, it remains infected and continues to attempt to infect its neighbors in the next round and subsequent rounds until it recovers. Once u recovers, it can no longer be infected. Obviously, after a sufficiently long time, all infected nodes will be recovered, and nodes can only be either susceptible or recovered. From the applicational perspective, we are interested in the number of the nodes *that have been infected* (e.g., in the examples in the previous paragraph, the advertiser immediately receives benefits when the users pay the subscription fees/membership fees). Equivalently, we are interested in the number of the *recovered* at the end of the cascade.

Plausible similarity between IC and SIR models. Previous work has observed the similarity between IC and SIR (see, e.g., Chapter 8.2 in Chen [2020]). In the SIR model, the probability that node u infects a neighbor v in some round is given by

$$p_{u,v} = \sum_{t=1}^{\infty} \gamma_u (1 - \gamma_u)^{t-1} (1 - (1 - \beta_{u,v})^t). \quad (1)$$

Here, $\gamma_u (1 - \gamma_u)^{t-1}$ represents the probability of node u recovering in round t , and $(1 - (1 - \beta_{u,v})^t)$ is the probability of node u successfully infecting v in at least one of the t rounds. By considering $p_{u,v}$ in Equation (1) as the IC parameter, we can observe the similarity in the cascading processes between both models. In the SIR model, we can “aggregate” the infection attempts along each edge over multiple rounds, and the overall probability becomes the IC parameter.

However, this observation raises a question and thus leads to the distinction between the IC model and the SIR model. In the SIR model, due to this aggregation, infections along the incident edges to a node are no longer independent. Intuitively, the event of u successfully infecting one of its neighbors v_1 is positively correlated with the event of u infecting another neighbor v_2 , as success on one edge increases the likelihood of u not recovering for a longer period, thus enhancing the probability of success on another edge. This dependency creates a difference between the two models. Our objective is to explore whether this additional dependency on outgoing edges enhances or hampers the spread of information. Consequently, we consider the SIR model as an outgoing-edges-dependent variant of the IC rather than following the original SIR definition.

From the above analysis, we can interpret the SIR model by the IC model if the above dependency can be ignored. Past literature has noticed the similarity and this seemingly “slight” difference between the two models. However, it is unclear how significant this difference is. For example, given the same graph and the same seed set, and assuming that the parameters setting in IC and SIR satisfy Equation (1), is the spread of the seeds in these two models substantially different?

Influence maximization with SIR model. The *influence maximization problem* (InfMax), proposed by Kempe et al. [2015], Richardson and Domingos [2002], Domingos and Richardson [2001], is the problem of selecting a set of “influencers” (also known as *seeds*) in social networks to maximize the expected number of influenced agents. The InfMax problem has attracted remarkable attention from researchers due to its wide range of applications, including social advertising [Camarero and San José, 2011, Domingos and Richardson, 2001, Richardson and Domingos, 2002], product adoption [Brown and Reingen, 1987, Bass, 1976, Mahajan et al., 1990, Lappas et al., 2011], disease analysis [Zhan et al., 2018], rumor control [Wu and Pan, 2017] and social computing [Liu et al., 2023]. More comprehensive literature reviews can be found in books [Chen, 2020, Chen et al., 2022a] and survey [Li et al., 2018].

The InfMax problem with the IC model is well-studied. In the first paper where the model is proposed, Kempe et al. [2015] show that a simple greedy algorithm achieves a $(1 - 1/e)$ -approximation, and no polynomial time $(1 - 1/e + \epsilon)$ -approximation algorithm exists assuming $P \neq NP$. After this, extensive work has focused on designing faster algorithms while keeping the theoretical approximation guarantee [Borgs et al., 2014, Chen et al., 2012, Goyal et al., 2011, Tang et al., 2015, Leskovec et al., 2007, Kempe et al., 2015]. One of the most successful types of such algorithms is based on *reverse-reachable sets* [Borgs et al., 2014, Tang et al., 2014, 2015, Chen, 2018], which yields a near-linear time algorithm with the $(1 - 1/e)$ approximation ratio.

However, for those epidemic models including the SIR model, most of the existing results have focused on the *dynamic* of these epidemic models and analyzed equilibrium states [Sene, 2020, Kabir et al., 2019, Ehrhardt et al., 2019, Long and Wang, 2020, Kumar et al., 2020]. However, few studies have explored them *in the context of influence maximization*. On the other hand, maximizing the number of nodes that *have been infected at least once* remains a natural problem in multiple real-world applications. For example, in viral marketing, advertisers receive benefits or payments based on nodes’ infection, irrespective of subsequent recoveries. Nonetheless, nodes’ recoveries can negatively affect the cascading process. Therefore, advertisers must consider this factor to attain a more comprehensive understanding of the cascade, enabling them to identify the optimal initial influencers.

We have previously seen the similarity and the subtle difference between the IC model and the SIR model. Regarding InfMax, are the seeding strategies considerably different for the two models even if the parameters satisfy Equation (1)? If the difference is insignificant, the InfMax algorithms for the IC model can be directed applied to the SIR model by reducing the SIR model to the IC model based on Equation (1). Otherwise, we should look for algorithms that are specifically designed for the SIR model.

1.1 Our Contributions

Stronger propagation effect in the IC model. As mentioned earlier, in the SIR model, through Equation (1), we can compute the probability that a vertex u “eventually” infects v before its recovery and obtain an “aggregated probability” $p_{u,v}$. This establishes an equivalence between the SIR model and the IC model, except that the events that the infections succeed along different edges become dependent in the SIR model. We intensively study how this seemingly minor difference in dependency affects the influence spread and the seeding strategy.

Firstly, in Sections 3 and 4, we show that this dependency can only *harm* the influence spread. Specifically, we prove the following novel observation: when comparing the two models, given the same graph, the same seed set, and the cascade model parameters related by Equation (1), the expected number of infected vertices under the IC model is always weakly larger than that under the SIR model. This is proved by developing a novel coupling method.

Furthermore, we show that the above gap in the expected number of infections can be made arbitrarily large in some instances. In addition, we also observed that, in certain networks, the optimal seeding strategies for the SIR and IC models are different, leading to significant differences in propagation outcomes. This motivates the need for designing algorithms specifically for the SIR model.

Approximation algorithms for the SIR model and its variants. We remark that the influence spread functions for all the proposed epidemic models based on SIR are *submodular* functions. This implies that the simple greedy algorithm achieves a $(1 - 1/e)$ -approximation. However, the conventional greedy algorithm based on Monte-Carlo sampling is known to be slow in practice. We adapt those reverse-reachable-set-based algorithms to the SIR setting, which yields a $(1 - 1/e - \epsilon)$ -approximation algorithm with probability at least $1 - n^{-\ell}$ for graphs with n nodes and parameters ϵ, ℓ , where the algorithm’s running time is *near-linear* in the number of nodes n .

1.2 Related Work

Many of the related papers have been discussed previously. In this section, we discuss further related work on the algorithmic aspect.

In the most general case, approximating InfMax to within a factor of $n^{1-\epsilon}$ is NP-hard [Kempe et al., 2015]. The strong inapproximability comes from the *nonsubmodularity* of the diffusion models: strong inapproximability results are known for InfMax even under very specific simple nonsubmodular diffusion models; as a result, researchers focus on heuristics (see, e.g., [Kempe et al., 2015, Chen, 2009, Angell and Schoenebeck, 2017, Schoenebeck and Tao, 2019, Schoenebeck et al., 2022]). On the other hand, when dealing with *submodular* diffusion models, a simple greedy algorithm achieves an $(1-1/e)$ -approximation: specifically, the global influence function $\sigma(\cdot)$ is a submodular set function if the diffusion model is submodular [Mossel and Roch, 2010], so the greedy algorithm achieves an $(1-1/e)$ -approximation [Nemhauser et al., 1978]. The approximation guarantee can be even slightly better than $(1-1/e)$ if the network is undirected [Khanna and Lucier, 2014, Schoenebeck et al., 2020]. On the inapproximability side, it is known that the $(1-1/e)$ -approximation cannot be improved for the IC model and directed graphs, unless $P = NP$ [Kempe et al., 2015]. Weaker APX-hardness results are known for undirected graphs and other submodular models such as the *linear threshold model* [Schoenebeck and Tao, 2020].

Unfortunately, the standard greedy algorithm is limited by its scalability, and therefore a large number of InfMax algorithms have been designed and tested on real networks. As a result, numerous solutions have been developed to optimize the efficiency of reaching the broadest audience possible on a massive network.

Various heuristic metrics have been developed based on the topological attributes of nodes. For example, closeness centrality measures the importance of each node by computing the reciprocal of its average distance from other nodes [Sabidussi, 1966]. Degree centrality, on the other hand, quantifies the influence of a node based on the number of its direct neighbors [Freeman, 1978]. For instance, the DegDis [Chen et al., 2009] measures the influence of each node by iteratively selecting the nodes with the highest value that based on degrees, then discount the seeds' neighbors to obtain k seeds. A similar idea was applied in the VoteRank⁺⁺ algorithm [Liu et al., 2021], which utilizes a voting mechanism to measure the influence of nodes in networks. After selecting the node with the highest *score*, the VoteRank⁺⁺ discounts the *voting ability* of the seed node's neighbors to reduce the overlap of influence between seed nodes. This enables the influence of the seed nodes to be spread as widely as possible.

However, most of the existing techniques either sacrifice approximation guarantees for practical efficiency, or the other way around. By leveraging submodularity, the CELF algorithm has been developed to efficiently handle large-scale problems. It achieves near-optimal placements while being 700 times faster than a simple greedy algorithm [Leskovec et al., 2007]. The methods in references [Borgs et al., 2014, Chen et al., 2012, Goyal et al., 2011, Tang et al., 2015, Kempe et al., 2015] that provide $(1-1/e-\epsilon)$ -approximation algorithms with a cost that is lower than greedy method.

One notable approach among these methods is the IMM algorithm (Influence Maximization with Martingales), introduced by Tang et al. [2015]. This algorithm operates with an expected time complexity of $O((k+l) \cdot (n+m) \cdot \log n/\epsilon^2)$ and provides an $(1-1/e-\epsilon)$ -approximation with a probability of at least $1-1/n^\ell$ under the triggering model. It addresses InfMax challenges by employing a martingale method, specifically estimating the number of reverse reachable sets. This feature allows IMM to significantly reduce redundant computations that were deemed unavoidable in the reference [Tang et al., 2014].

Other perspectives on studying the InfMax problem, such as learning-based, adaptivity, data-driven, and reinforcement-learning-based approaches, are discussed in references [Wu et al., 2019, Peng and Chen, 2019, Chen and Peng, 2019, D'Angelo et al., 2020, Li et al., 2021, Chen et al., 2022b, Kong et al., 2023, Ma et al., 2022, Li et al., 2022, D'Angelo et al., 2023].

1.3 Structure of This Paper

In Section 2, we define the two diffusion models studied and the influence maximization problem. In Section 3, we discuss the live-edge graph formulation of the IC and SIR models, and we adapt the reverse-reachable set technique to the SIR model. These will be used in all the later sections. Our results for the theoretical comparison of the IC and SIR models are in Section 4. In Section 5, we discuss the algorithm design from the aspect of the InfMax problem with the SIR model.

2 Model and Preliminaries

A social network can be represented as a directed graph $G = (V, E)$ with n nodes (i.e., *users*) and m directed edges (i.e., *social connections* between *users*). For any directed edge $(u, v) \in E$, we say (u, v) is an incoming edge (resp. outgoing edge) of v (resp. u). We also call u an incoming neighbor of v and v an outgoing neighbor of u .

Definition 1 (Diffusion Model and Influence Spread [Kempe et al., 2015]). *Given a social network (directed graph) $G = (V, E)$, a **diffusion model** Γ is a (possibly random) function that maps from a vertex set S (the seeds that are initially infected) to a vertex set $\Gamma_G(S)$ (the set of influenced vertices at the end of the spreading). We omit the subscript G when there is no confusion. Denote by $\sigma(S) = \mathbf{E}[|\Gamma(S)|]$ the expected number of vertices influenced by S .*

The goal of the *influence maximization* problem (InfMax) is to select at most k nodes as *seeds* to maximize the number of *influenced* nodes on the social network G .

Definition 2 (Influence Maximization [Kempe et al., 2015]). *Given a social network (directed graph) $G = (V, E)$, a diffusion model Γ , and a positive integer k , the objective of influence maximization is to select a subset $S \subseteq V$ with $|S| \leq k$ that maximizes the expected influence spread $\sigma(S)$.*

2.1 Independent Cascade Model

In the Independent Cascade (IC) model [Kempe et al., 2015], the nodes could be *active* or *inactive* in a given directed graph $G = (V, E)$. A node $v \in V$ could be activated by each of its incoming active neighbors independently. More precisely, each directed edge $e = (u, v) \in E$ is associated with an activation probability $p_e = p_{u,v} \in [0, 1]$. The influence spread of an active seed set $S \subseteq V$ unfolds in discrete timestamps as follows.

1. At timestamp 0, only nodes in S are active.
2. At each timestamp $t = 1, 2, \dots$, each newly activated node u from the previous timestamp gets one chance to activate its inactive outgoing neighbors; and for each inactive outgoing neighbor v , u tries to activate v with a probability $p_{u,v}$. The attempts to activate neighbors are independent of each other. If multiple incoming neighbors of an inactive node attempt to activate it, each attempt is considered separately with its own probability.
3. The diffusion process terminates when no inactive node gets activated in a timestamp.

In the above process, once a node becomes active, it remains active throughout. When we are considering the IC model, i.e., $\Gamma = \text{IC}_{\mathbf{p}}$ where $\mathbf{p} = \{p_e\}_{e \in E}$ in Definition 1, $\text{IC}_{\mathbf{p}, G}(S)$ is the set of active nodes at the end of the above diffusion process.

In Kempe et al. [2015], it is shown that the influence spread of the IC model can be simulated by evaluating the number of *reachable* nodes from the seed set in the *live-edge graph*. To be specific, the random live-edge graph $\mathcal{G}_{\text{IC}}(G, \mathbf{p})$ corresponding to the instance (G, \mathbf{p}) under the IC model is generated by including each directed edge $e \in E$ in G with probability p_e . Each node v is active if it is reachable from the seed set S , that is, there exists a directed path from some nodes $v \in S$ to u in the live-edge graph. More discussions about live-edge graphs can be found in Section 3.

2.2 Susceptible-Infected-Recovered Model

In the Susceptible-Infected-Recovered Model (SIR) model [Kermack and McKendrick, 1927], the nodes could be *susceptible*, *infected*, or *recovered*. The SIR diffusion process is characterized by a directed graph $G = (V, E)$ together with two sets of parameters $\beta = \{\beta_e\}_{e \in E}$ and $\gamma = \{\gamma_v\}_{v \in V}$, where each node $v \in V$ is assigned a recovery probability $\gamma_v \in (0, 1]$ and each directed edge $e = (u, v)$ is associated with an infection probability $\beta_e = \beta_{u,v} \in (0, 1]$. The influence spread of an infected seed set $S \subseteq V$ unfolds in discrete timestamps as follows:

1. At timestamp 0, all nodes in the seed set S are initially infected, while the remaining nodes are considered susceptible.

2. At each timestamp $t = 1, 2, \dots$, each node u that is infected at timestamp t performs the following operations sequentially:
 - for each susceptible outgoing neighbors v , u infects v with probability $\beta_{u,v}$;
 - u gets recovered with a recovery probability γ_u and remains infected otherwise.
3. The diffusion process terminates when all nodes are either recovered or susceptible.

When we are considering the SIR model, i.e., $\Gamma = \text{SIR}_{\beta,\gamma}$ in Definition 1, $\text{SIR}_{\beta,\gamma,G}(S)$ is the set of recovered nodes at the end of the above diffusion process.

Remark. *It is implied that once a node becomes recovered in the SIR model, it can never be infected again or infect other nodes. Note that all infected nodes will eventually be recovered after a sufficiently long time.*

We also consider the spread of influence within a specific time frame T in the SIR model, referred to as the *Truncated Susceptible-Infected-Recovered* (TSIR) Model. In this model, with a seed set $S \subseteq V$ infected at time 0, the diffusion process unfolds as described earlier but stops at time T . The influence spread $\text{TSIR}_{\beta,\gamma,T,G}(S)$ is defined as the number of nodes that have been infected by time T . Thus, when taking $\Gamma = \text{TSIR}_{\beta,\gamma,T}$, the “influenced vertices” in Definition 1 are those that are infected or recovered.

3 Live-edge Graph and Reverse Reachable Set

Similar to the equivalent formulation proposed by Kempe et al. [2015] for the IC model, we demonstrate that the influence spread of the diffusion models we consider can be formulated using a model-specific live-edge graph. This live-edge graph formulation allows us to study the models using the unified characterization of the *reverse reachable set* [Borgs et al., 2014] in our later discussion.

3.1 Live-edge Graph Formulation

The live-edge graph of a diffusion model is a random spanning sub-graph of G that reflects the diffusion behavior. Specifically, each edge in the original network is either “*live*” (active) or “*blocked*” (inactive), based on the model’s spread probabilities, and the live-edge graph is the subgraph consisting of live edges. Roughly speaking, each edge (u, v) is live (included in the live-edge graph) with a probability, which represents the likelihood of u activating v during the influence spread period. Thus, a live-edge graph is an equivalent representation of a spreading process on G based on a diffusion model, and it serves as a sampling graph that captures one possible propagation of the model. By evaluating the number of *reachable* nodes from a given seed set S in the *live-edge graph*, we can simulate the spreading ability of S in the diffusion process.

Definition 3 (Live-edge Graph Formulation). *Given a social network (directed graph) $G = (V, E)$ with the diffusion model Γ , we say Γ is a live-edge graph diffusion model if there exists a measure μ over the collection of (possibly edge-weighted) spanning sub-graphs of G , such that the influence spread $\sigma(S)$ equals the expected number of reachable nodes from S in the live-edge graph \mathcal{G} sampled from μ for any seed set $S \subseteq V$.*

For convenience, we abuse \mathcal{G} to represent the edge set $E(\mathcal{G})$ of the live-edge graph \mathcal{G} and thus $e \in \mathcal{G}$ means that e is one of the edges in \mathcal{G} for any $e \in E$ in subsequent discussion.

In the following, we introduce the live-edge graph formulation for the SIR model. For the TSIR model, the live-edge graph characterization can be found in Section 3.1.2.

3.1.1 The Live-edge Graph for the SIR Model

The influence spread of seed nodes in the SIR model on instance $(G = (V, E), \beta, \gamma)$ can be characterized by the number of reachable nodes in the live-edge graph

$$\mathcal{G}_{\text{SIR}} = \mathcal{G}_{\text{SIR}}(G, \beta, \gamma) = \mathcal{G}_{\text{SIR}}(G, \{\mathbf{R}_v\}_{v \in V}, \{\mathbf{I}_e\}_{e \in E})$$

induced by a collection of independent variables

$$\mathbf{R}_v = (R_{v,1}, R_{v,2}, \dots), \quad \text{and} \quad \mathbf{I}_e = (I_{e,1}, I_{e,2}, \dots),$$

where $R_{v,t} \sim \text{Bern}(\gamma_v)$ for any $v \in V, t \in \mathbb{N}^+$ and $I_{e,t} \sim \text{Bern}(\beta_e)$ for any $e \in E, t \in \mathbb{N}^+$ are Bernoulli random variables. Here, $R_{u,t} = 1$ denotes that u is recovered at the t -round after u 's infection, and $R_{v,t} = 0$ otherwise. Similarly, $I_{(u,v),t}$ is the indicator random variable for the event that u successfully infects v at the t -th round after u is infected. Specifically, each directed edge $e = (u, v) \in E$ is included in \mathcal{G}_{SIR} if there exists some $t^* \geq 1$ such that $I_{e,t^*} = 1$ and $R_{u,[t^*-1]} = (R_{u,1}, R_{u,2}, \dots, R_{u,t^*-1})$ is a sequence of zeros with length $t^* - 1$. In other words, the influence spread from node u to node v succeeds at timestamp t^* before the node u gets recovered, and the edge e represents a successful infection event between nodes u and v that could have occurred. Here, we say a node v is reachable from u in \mathcal{G}_{SIR} if there exists a directed path from u to v in \mathcal{G}_{SIR} . An example is illustrated below.

Example 1. Consider a graph $G = (V, E)$ with $V = \{u, v, w\}$ and $E = \{(u, v), (u, w)\}$. Assume we have sampled indicator random variables $\mathbf{R}_u = (R_{u,1}, R_{u,2}, \dots) = (0, 0, 0, 1, \dots)$, $\mathbf{I}_{(u,v)} = (I_{(u,v),1}, I_{(u,v),2}, \dots) = (0, 0, 1, \dots)$, and $\mathbf{I}_{(u,w)} = (I_{(u,w),1}, I_{(u,w),2}, \dots) = (0, 0, 0, 0, 1, \dots)$. In this example, u is recovered at round 4. The infection from u to v is successful at round 3, and the infection from u to w is successful at round 6. Therefore, u can successfully infect v before u 's recovery, while u cannot infect w before its recovery. Correspondingly, in the live-edge graph, (u, v) is live and (u, w) is blocked, i.e., $(u, v) \in \mathcal{G}_{\text{SIR}}$ and $(u, w) \notin \mathcal{G}_{\text{SIR}}$.

The proof of the following proposition is straightforward: this is just a rephrasing of the same stochastic process. It is deferred to Appendix A.

Proposition 4. \mathcal{G}_{SIR} defined above is a live-edge graph formulation of $\text{SIR}_{\beta, \gamma}$, namely,

$$\sigma_{\text{SIR}}(S) = \mathbf{E}[\text{the number of reachable nodes from } S \text{ in } \mathcal{G}_{\text{SIR}}].$$

As mentioned in Section 1, we are interested in comparing the two diffusion processes corresponding to IC and SIR respectively with the equal marginal probability for u successfully infecting v along each edge (u, v) . Equation (1) ensures this, which is described in the proposition below (whose proof is straightforward).

Proposition 5. Given any directed graph $G = (V, E)$ together with the diffusion models $\text{IC}_{\mathbf{p}}$ and $\text{SIR}_{\beta, \gamma}$ where the parameters satisfying Equation (1), it holds that $\Pr[e \in \mathcal{G}_{\text{IC}}] = \Pr[e \in \mathcal{G}_{\text{SIR}}]$ for each $e \in E$.

3.1.2 The Live-edge Graph for the TSIR Model

Given a specific time threshold T , the influence spread of seed nodes in the TSIR diffusion model on instance $(G = (V, E), \beta, \gamma, T)$ can be characterized by the number of reachable nodes in the live-edge graph

$$\mathcal{G}_{\text{TSIR}} = \mathcal{G}_{\text{TSIR}}(G, \beta, \gamma, T) = \mathcal{G}_{\text{TSIR}}(G, \{\mathbf{R}_v\}_{v \in V}, \{\mathbf{I}_e\}_{e \in E}, T)$$

induced by a collection of independent Bernoulli random variables, similar to that of the SIR model together with the weight on the edges: an edge $e = (u, v) \in E$ is included in $\mathcal{G}_{\text{TSIR}}$ with infection span $w_e = w_{u,v} = t^*$ if t^* is the smallest positive integer satisfying $I_{e,t^*} = 1$ and $R_{u,[t^*-1]}$ is a sequence of zeros with length $t^* - 1$.

The infection span of each edge (u, v) captures the timestamps needed to influence propagation from u to v . We call the node v is T -reachable from u in $\mathcal{G}_{\text{TSIR}}$ if there exists a directed path $P = (u_1 = u, u_2, \dots, u_\ell = v)$ in $\mathcal{G}_{\text{TSIR}}$ such that $\sum_{i \in \ell-1} w_{u_i, u_{i+1}} \leq T$. The influenced nodes of any seed set $S \subseteq V$ on the graph $G = (V, E)$ then equals the number of T -reachable nodes from S in $\mathcal{G}_{\text{TSIR}}$. An example is illustrated below.

Example 2. Consider a graph $G = (V, E)$ with $V = \{u, v, w\}$ and $E = \{(u, v), (u, w), (v, w)\}$. Assume we have sampled indicator random variables $\mathbf{R}_u = (R_{u,1}, R_{u,2}, \dots) = (0, 0, 0, 1, \dots)$, $\mathbf{I}_{(u,v)} = (I_{(u,v),1}, I_{(u,v),2}, \dots) = (0, 0, 1, \dots)$, $\mathbf{I}_{(u,w)} = (I_{(u,w),1}, I_{(u,w),2}, \dots) = (0, 0, 0, 0, 1, \dots)$, $\mathbf{I}_{(v,w)} = (I_{(v,w),1}, I_{(v,w),2}, \dots) = (0, 1, \dots)$, and we set $T = 4$. In the above example, u is recovered at round 4, u infect v at round 3, u infect w at round 6, and v infect w at round 2. In the graph $\mathcal{G}_{\text{TSIR}}$, the edges (u, v) and (v, w) have infection spans of 3 and 2 respectively. Consequently, within the time threshold $T = 4$, u can successfully infect v , but it will fail to infect w due to the shortest path from u to w having a total weight of 5.

Similarly, we can prove the following live-edge graph characterization for the TSIR model, the proof of which is similar to that of proposition 4.

Proposition 6. Given a social network (directed graph) $G = (V, E)$ with the $\text{TSIR}_{\beta, \gamma, T}$ diffusion model, we have for any seed set $S \subseteq V$,

$$\sigma_{\text{TSIR}}(S) = \mathbf{E}[\text{the number of } T\text{-reachable nodes from } S \text{ in } \mathcal{G}_{\text{TSIR}}].$$

3.2 Reverse Reachable Set Characterization

The influence spread of the aforementioned models can be characterized by the notion of the *reverse reachable set* [Borgs et al., 2014] under the live-edge graph formulation. When considering a live-edge graph diffusion model, we sometimes use \mathcal{G} to represent its diffusion process instead of Γ . The definition of the reverse reachable set can be stated as follows.

Definition 7 (Reverse Reachable Set). *Given a directed graph $G = (V, E)$ with the live-edge graph \mathcal{G} , the reverse reachable set of a node $v \in V$, denoted by $\text{RR}_{\mathcal{G}}(v)$, is the set of all nodes in \mathcal{G} that can reach v . Furthermore, let $\text{RR}_{\mathcal{G}}$ be the random set $\text{RR}_{\mathcal{G}}(v)$ with v selected uniformly at random from V .*

Proposition 8. *Given a directed graph $G = (V, E)$ with a live-edge graph diffusion model \mathcal{G} , the probability that the diffusion process from any seed set $S \subseteq V$ can influence a node v equals the probability that S overlaps with the set $\text{RR}_{\mathcal{G}}(v)$, i.e., $\Pr[S \cap \text{RR}_{\mathcal{G}}(v) \neq \emptyset]$. Furthermore, the influence spread satisfies*

$$\sigma(S) = \sum_{v \in V} \Pr[S \cap \text{RR}_{\mathcal{G}}(v) \neq \emptyset] = |V| \cdot \Pr[S \cap \text{RR}_{\mathcal{G}} \neq \emptyset].$$

In later discussion, we sometimes use $\text{RR}_{\text{IC}}(v)$ (RR_{IC} , resp.) to denote the reverse reachable set of a node v (random reverse reachable set, resp.) corresponding to the live-edge graph \mathcal{G}_{IC} for simplicity. The notations $\text{RR}_{\text{SIR}}(v)$, $\text{RR}_{\text{TSIR}}(v)$, RR_{SIR} , and RR_{TSIR} are defined similarly.

4 Theoretical Comparison between the IC and SIR Models

As discussed in Section 1, we can “aggregate” the infection attempts in multiple rounds along each edge in the SIR model so that the SIR model and the IC model can be related by Equation (1). However, if we view the SIR model in this way, infections across different outgoing edges of a node are correlated. In this section, we prove that this correlation *negatively* affects the cascade: given a graph G and a set of seeds S and setting the parameters of IC and SIR to satisfy Equation (1), the influence spread of IC dominates SIR. Moreover, we further show that the differences between IC and SIR lead to different seeding strategies.

We first show the positive correlation property with respect to the occurrence of the edges in the SIR model (Section 4.1). Together with the reverse reachable set characterization of influence spread, we demonstrate that the influence spread in the IC model dominates the one in the corresponding SIR model conditioned on the comparable spreading ability on each edge by a coupling between the reverse reachable set (Theorem 10 in Section 4.2). Furthermore, in certain scenarios, we find that the IC model can significantly dominate the SIR model. We delve deeper into these scenarios to claim that the influence of IC could significantly dominate SIR, which further implies different seeding strategies.

4.1 Positive Correlation in the SIR Model

According to the live-edge graph formulation of the SIR model, the positive correlation can be described as follows: the probability of an edge being included in the live-edge graph decreases if other edges in the underlying graph G are not included.

Lemma 9. *Given a directed graph $G = (V, E)$ with the diffusion model $\text{SIR}_{\beta, \gamma}$, we have*

$$\Pr[e \in \mathcal{G}_{\text{SIR}} \mid E' \cap \mathcal{G}_{\text{SIR}} = \emptyset] \leq \Pr[e \in \mathcal{G}_{\text{SIR}}]$$

for any $E' \subseteq E$ and $e \in E \setminus E'$.

A tiny example is helpful to understand Lemma 9. Given $G = (V, E)$ with $V = \{u, v, w\}$, $E = \{(u, v), (u, w)\}$, and letting $e = (u, v)$ and $E' = \{(u, w)\}$, Lemma 9 says that the event $(u, w) \notin \mathcal{G}_{\text{SIR}}$ makes the edge (u, v) less likely to be live. The proof of this lemma is deferred to Appendix A. Intuitively, in the above example, if knowing (u, w) is not live, u is more likely to recover at earlier rounds, which decreases the chance that (u, v) is live. In general, knowing a set of edges fails to be live makes an edge less likely to be live.

Remark. *The dependency exists only on the outgoing edges from the same vertex. It is obvious from the definition of SIR that the events $e_1 \in \mathcal{G}_{\text{SIR}}$ and $e_2 \in \mathcal{G}_{\text{SIR}}$ are independent if e_1 and e_2 are not outgoing edges of the same vertex.*

To show that IC dominates SIR given the same seed set and with parameters satisfying Equation (1), a natural idea is to couple the two spreading processes such that the set of infected vertices in the SIR process is a subset of the set of infected vertices in the IC process. However, in the following example, we demonstrate that such a coupling is unlikely to exist.

Consider a seed set with a single seed s that has many outgoing neighbors. In the IC model, the events that s successfully infects its neighbors are independent. In the SIR model, due to Equation (1), s infects each neighbor with the same probability as in the IC model. Thus, the expected number of infected neighbors is the same in both models due to the linearity of expectation. Intuitively, due to the positive correlation, in the SIR model, the number of infected neighbors is more likely to be either very small or very large. However, because of the same expectation, it is impossible to find a coupling such that the set of infected neighbors in SIR is a subset of the set of infected neighbors in IC. In fact, from this example, it is not even intuitively clear that IC is superior to SIR.

In the next section, we will use a coupling on sampling the reverse-reachable sets of an arbitrary vertex v . We will show that viewing the cascade in such a “backward” way helps us better understand the relationship between the two models.

4.2 IC Dominating SIR

Given a directed graph $G = (V, E)$, we rigorously prove that the influence spread of any seed set in the IC model dominates that of the SIR model, under the assumption that the parameters satisfy Equation (1).

Theorem 10. *Given any directed graph $G = (V, E)$ together with the diffusion models $\text{IC}_{\mathbf{p}}$ and $\text{SIR}_{\beta, \gamma}$ where the parameters satisfy Equation (1), we have for any set $S \subseteq V$,*

$$\sigma_{\text{IC}}(S) \geq \sigma_{\text{SIR}}(S).$$

According to the linearity of the expectation and the reverse reachable set characterization of the influence spread Proposition 8, it suffices to show the following lemma.

Lemma 11. *Given any directed graph $G = (V, E)$ together with the diffusion models $\text{IC}_{\mathbf{p}}$ and $\text{SIR}_{\beta, \gamma}$, where the parameters satisfy Equation (1), we have for any seed set $S \subseteq V$ and any node $v \in V$,*

$$\Pr[S \cap \text{RR}_{\text{IC}}(v) \neq \emptyset] \geq \Pr[S \cap \text{RR}_{\text{SIR}}(v) \neq \emptyset].$$

The lemma above straightforwardly implies Theorem 10.

Proof of Theorem 10. According to Proposition 8, we have

$$\sigma_{\text{IC}}(S) = \sum_{v \in V} \Pr[S \cap \text{RR}_{\text{IC}}(v) \neq \emptyset] \geq \sum_{v \in V} \Pr[S \cap \text{RR}_{\text{SIR}}(v) \neq \emptyset] = \sigma_{\text{SIR}}(S)$$

where the inequality follows from Lemma 11. □

It now remains to prove Lemma 11.

4.2.1 Some Intuitions for the Correctness of Lemma 11.

To prove Lemma 11, considering an arbitrary fixed v , we define a coupling between \mathcal{G}_{IC} and \mathcal{G}_{SIR} such that $\text{RR}_{\text{SIR}}(v) \subseteq \text{RR}_{\text{IC}}(v)$. The existence of such a coupling immediately implies the lemma. It then remains to define such a coupling. We first describe the high-level ideas as follows.

The edges in both \mathcal{G}_{IC} and \mathcal{G}_{SIR} are revealed on a need-to-know basis. Specifically, the edges are revealed in a reverse Breadth-First-Search process: let U denote the set of vertices that can reach vertex v , initialized as $U = \{v\}$; in each iteration, for every vertex x that has out-neighbors in U , we reveal the corresponding outgoing edges of x ; if one of these outgoing edges is live, then x is included in U . In addition, we can

maintain an in-arborescence (a directed tree rooted at v where each edge is from the child to the parent) containing the reverse reachable nodes of v : if the node x has at least one outgoing edge connecting to U that is live, we pick an arbitrary such live edge and include it in the in-arborescence. Note that, after this process, unrevealed edges have no effect on $\text{RR}_{\text{IC}}(v)$ or $\text{RR}_{\text{SIR}}(v)$. We couple the two reverse Breadth-First-Search processes for $\text{RR}_{\text{IC}}(v)$ and $\text{RR}_{\text{SIR}}(v)$ respectively such that the in-arborescence for the former is a superset of the in-arborescence for the latter. The fact that each node in an in-arborescence has an out-degree at most 1 ensures that this is always possible. This is better illustrated by the following example.

Suppose at a certain stage of the Breadth-First-Search process where, in both IC and SIR processes, U is the set of vertices that are already in the in-arborescence, and suppose now we are revealing the outgoing edges of a vertex $x \notin U$ to see if x is in the in-arborescence. Suppose, for example, $y_1, y_2, y_3 \in U$ are all the outgoing neighbors of x that belong to U . If at least one of (x, y_1) , (x, y_2) , and (x, y_3) is live in the SIR process, then x is included in U in the next iteration. Our coupling ensures that x is also included in U in the IC process. To see this, taking an example where $(x, y_2), (x, y_3) \in \mathcal{G}_{\text{SIR}}$ and $(x, y_1) \notin \mathcal{G}_{\text{SIR}}$, which happens with probability $\Pr[(x, y_1) \notin \mathcal{G}_{\text{SIR}}] \cdot \Pr[(x, y_2) \in \mathcal{G}_{\text{SIR}} \mid (x, y_1) \notin \mathcal{G}_{\text{SIR}}] \cdot \Pr[(x, y_3) \in \mathcal{G}_{\text{SIR}} \mid (x, y_1) \notin \mathcal{G}_{\text{SIR}}, (x, y_2) \in \mathcal{G}_{\text{SIR}}]$. The live edge with the smallest index, which is (x, y_2) in this case, is included in the in-arborescence, and x is included in U . We consider these three probabilities in the IC model. For the first, we have $\Pr[(x, y_1) \in \mathcal{G}_{\text{SIR}}] = \Pr[(x, y_1) \in \mathcal{G}_{\text{IC}}]$ due to Equation (1). For the second, we have

$$\begin{aligned} \Pr[(x, y_2) \in \mathcal{G}_{\text{SIR}} \mid (x, y_1) \notin \mathcal{G}_{\text{SIR}}] &\leq \Pr[(x, y_2) \in \mathcal{G}_{\text{SIR}}] && \text{(Lemma 9)} \\ &= \Pr[(x, y_2) \in \mathcal{G}_{\text{IC}}] && \text{(Equation (1))} \\ &= \Pr[(x, y_2) \in \mathcal{G}_{\text{IC}} \mid (x, y_1) \notin \mathcal{G}_{\text{IC}}]. && \text{(Independence in IC)} \end{aligned}$$

By coupling the events for the first two edges (x, y_1) and (x, y_2) , we already ensure that x is included in U in the IC process as well. Notice that, for the third probability, although the relationship between

$$\Pr[(x, y_3) \in \mathcal{G}_{\text{SIR}} \mid (x, y_1) \notin \mathcal{G}_{\text{SIR}}, (x, y_2) \in \mathcal{G}_{\text{SIR}}]$$

and

$$\Pr[(x, y_3) \in \mathcal{G}_{\text{IC}} \mid (x, y_1) \notin \mathcal{G}_{\text{IC}}, (x, y_2) \in \mathcal{G}_{\text{IC}}]$$

cannot be implied by Lemma 9, we have already included x in U regardless of the status of (x, y_3) . Even if the conditional probability that (x, y_3) is live for SIR is higher than it is for IC, this does not give SIR any advantages.

More generally, if x has many out-neighbors y_1, y_2, \dots, y_k in U and i is the smallest index such that (x, y_i) is live in the SIR process, by Lemma 9, the event that $(x, y_1), \dots, (x, y_{i-1})$ are blocked reduces the chance that (x, y_i) is live in the SIR process, while this event has no effect on the chance that (x, y_i) is live in the IC process. By coupling the event corresponding to the status of the first i edges, we can make x be included in U for the IC process whenever this happens in the SIR process. Although (x, y_i) being live may increase the chances of $(x, y_{i+1}), \dots, (x, y_k)$ being live in the SIR process, this does not give SIR any advantages against IC as x is already included in U due to the inclusion of (x, y_i) in the in-arborescence. The fact that we only need one live edge from x to U and the correlation property described in Lemma 9 make IC superior to SIR.

Notice that the main purpose of the example above is to give readers some intuitions. A rigorous proof follows next.

4.2.2 The Proof of Lemma 11.

Given any node $v \in V$ with the live-edge graph \mathcal{G} , we can determine the set $\text{RR}_{\mathcal{G}}(v)$ in a reverse Breadth-First-Search way, and the edges are revealed on a need-to-know basis. Specifically, let U denote the set of vertices that can reach vertex v , initialized as $U = \{v\}$ and $A \subseteq V \setminus U$ be the set of nodes that has out-neighbors in U . We repeat the following operations until there are no more nodes that can be added into U , i.e., $A = \emptyset$: select an arbitrary node $u \in A$, and reveal its outgoing edges to U in an arbitrary fixed order. Once there exists an outgoing edge occurs in \mathcal{G} , we update $U \leftarrow U \cup \{u\}$ and skip the remaining unrevealed edges as these edges will not affect the reverse reachable set. One can easily verify that $U = \text{RR}_{\mathcal{G}}(v)$ upon the termination of the process.

To show that IC dominates SIR, we design a coupling between the reverse reachable set realization processes of IC and SIR. As mentioned in Section 4.2, the coupling relies on the in-arborescence structure in the SIR process. This is because the probability of an outgoing edge occurring in \mathcal{G}_{SIR} is less than that in \mathcal{G}_{IC} given that it is the first live edge revealed (according to Lemma 9).

Based on the need-to-know principle, we maintain an in-arborescence in the SIR process and a live-edge sub-graph in IC such that the former is the subset of the latter, which implies that the reverse reachable set of IC is a superset of the corresponding set in SIR at each step. Specifically, let E_1 and E_2 be the random live edges in IC and SIR that have been revealed at each step. We also use $G_1 = (V, E_1)$ and $G_2 = (V, E_2)$ to denote the sub-graphs that consist of edges and vertices related to E_1 and E_2 , respectively. Moreover, the set RR_1 and RR_2 correspond to the reverse reachable nodes of v in $G_1 = (V, E_1)$ and $G_2 = (V, E_2)$, respectively. As one will see, G_2 forms an in-arborescence, and G_2 is always a subgraph of G_1 , which implies that $\text{RR}_2 \subseteq \text{RR}_1$ at each step.

Let A be the collection of nodes that have unrevealed outgoing edges pointing to RR_2 . At each round, we select a node $u \in A$ and reveal the unrevealed edges from u to RR_2 . We use E'_u to denote the set of outgoing edges of the node u that have been revealed in previous rounds, and $((u, u_1), \dots, (u, u_\ell))$ to denote the unrevealed outgoing edges of u with endpoints in RR_2 listed by the index order. We reveal the edges in $((u, u_1), \dots, (u, u_\ell))$ in order and stop revealing more edges once an edge is live. During the coupling process, for each unsampled edge $e = (u, u_j)$ where $j \in [\ell]$, we operates as follows:

1. Sampling $p \sim \text{Unif}[0, 1]$;
2. For IC, if $p \leq p_{u, u_j}$ then make e live in the live-edge graph \mathcal{G}_{IC} , $\text{RR}_1 \leftarrow \text{RR}_1 \cup \{u\}$, $E_1 \leftarrow E_1 \cup \{(u, u_j)\}$;
3. For SIR, if $p \leq \mathbf{Pr}[(u, u_j) \in \mathcal{G}_{\text{SIR}} \mid E'_u \cap \mathcal{G}_{\text{SIR}} = \emptyset]$ then make e live in the live-edge graph \mathcal{G}_{SIR} , $\text{RR}_2 \leftarrow \text{RR}_2 \cup \{u\}$, $E_2 \leftarrow E_2 \cup \{(u, u_j)\}$, skip the examination of the remaining edges;
4. Setting $E'_u \leftarrow E'_u \cup \{e\}$.

Once there are no more nodes that have out-neighbors in RR_2 , we reveal the whole live-edge graph on the unrevealed edge. Specifically, let \mathcal{G}_1 and \mathcal{G}_2 be the random live-edge graph by revealing the edges in $E \setminus (\bigcup_{u \in V} E'_u)$ according to the correct marginal distributions, respectively. The formal description of our coupling is presented in Algorithm 1. Note that the variable `flag` in Algorithm 1 is the indicator of whether there is an outgoing edge that is live.

The realization of the edges follows from the correct marginal distribution, which ensures the correctness of our live-edge graphs.

Lemma 12. *In Algorithm 1, \mathcal{G}_1 and \mathcal{G}_2 follow the distribution of \mathcal{G}_{IC} and \mathcal{G}_{SIR} , respectively.*

Proof. It is obvious that \mathcal{G}_1 follows the distribution of \mathcal{G}_{IC} since each edge $e \in E$ is included in \mathcal{G}_{IC} independently. We next show the same fact holds for \mathcal{G}_2 . Let $E' = \bigcup_{u \in V} E'_u$. It suffices to show that our coupling process maintains (E_2, E') with probability $\mathbf{Pr}[\mathcal{E}]$ where \mathcal{E} denote the event that $E_2 \subseteq \mathcal{G}_{\text{SIR}}$ and $(E' \setminus E_2) \cap \mathcal{G}_{\text{SIR}} = \emptyset$. We prove it by a structural induction with the satisfying induction basis $E_2 = E' = \emptyset$. For the induction step, we assume that $e = (u, u')$ is the next edge to be sampled given the current E_2 and E' . According to the coupling procedure, e is included with probability $\mathbf{Pr}[e \in \mathcal{G}_{\text{SIR}} \mid E'_u \cap \mathcal{G}_{\text{SIR}} = \emptyset]$. By definition, we have

$$\mathbf{Pr}[e \in \mathcal{G}_{\text{SIR}} \mid E'_u \cap \mathcal{G}_{\text{SIR}} = \emptyset] = \mathbf{Pr}[e \in \mathcal{G}_{\text{SIR}} \mid \mathcal{E}].$$

Combining with the induction hypothesis that (E_2, E') are obtained with $\mathbf{Pr}[\mathcal{E}]$, we add e to E_2 and remove e from E' with probability

$$\mathbf{Pr}[e \in \mathcal{G}_{\text{SIR}} \mid \mathcal{E}] \cdot \mathbf{Pr}[\mathcal{E}] = \mathbf{Pr}[(E_2 \cup \{e\}) \subseteq \mathcal{G}_{\text{SIR}}, (E' \setminus E_2) \cap \mathcal{G}_{\text{SIR}} = \emptyset].$$

The case when e is not included in the live-edge graph is similar, and the proof is complete. \square

By sharing the randomness on the realization of each edge in IC and SIR, we couple the propagation of the influence and maintain that $\text{RR}_1 \supseteq \text{RR}_2$ by the positive correlation property in the SIR model.

Algorithm 1: The reverse recursive coupling \mathcal{C}_v

Input: A directed graph $G = (V, E)$ with the parameters \mathbf{p} and β, γ , and a node $v \in V$.
Output: A pair of live-edge graph $\mathcal{G}_1, \mathcal{G}_2$.

- 1 Label an arbitrary order on the nodes and edges in G ;
- 2 $E_1 = E_2 \leftarrow \{\emptyset\}$ and $\text{RR}_1 = \text{RR}_2 \leftarrow \{v\}$;
- 3 $E'_u \leftarrow \emptyset$ for any $u \in V$;
- 4 **while** $A \leftarrow \{u \in V \setminus \text{RR}_2 \mid \exists u' \in \text{RR}_2, (u, u') \in E \setminus E'_u\}$ and $A \neq \emptyset$ **do**
- 5 Select the node $u \in A$ with the smallest index;
- 6 Let $((u, u_1), \dots, (u, u_\ell))$ be the directed edges not in E'_u with endpoints in RR_2 listed by the index order;
- 7 $j \leftarrow 0$, **flag** $\leftarrow 0$;
- 8 **repeat**
- 9 $j \leftarrow j + 1$;
- 10 Sample $p \sim \text{Unif}[0, 1]$;
- 11 $\text{RR}_1 \leftarrow \text{RR}_1 \cup \{u\}$, $E_1 \leftarrow E_1 \cup \{(u, u_j)\}$ when $p \leq p_{u, u_j}$;
- 12 $\text{RR}_2 \leftarrow \text{RR}_2 \cup \{u\}$, $E_2 \leftarrow E_2 \cup \{(u, u_j)\}$ and **flag** $\leftarrow 1$ when $p \leq \Pr[(u, u_j) \in \mathcal{G}_{\text{SIR}} \mid E'_u \cap \mathcal{G}_{\text{SIR}} = \emptyset]$;
- 13 $E'_u \leftarrow E'_u \cup \{(u, u_j)\}$;
- 14 **until** **flag** = 1 or $j = \ell$;
- 15 Let \mathcal{G}_1 and \mathcal{G}_2 be the random live-edge graph by revealing the edges in $E \setminus (\bigcup_{u \in V} E'_u)$ according to the correct marginal distributions, respectively;
- 16 **return** $(\mathcal{G}_1, \mathcal{G}_2)$.

Lemma 13. *Given any directed graph $G = (V, E)$ together with the diffusion models $\text{IC}_{\mathbf{p}}$ and $\text{SIR}_{\beta, \gamma}$, we have that*

$$\forall v \in V, \quad \text{RR}_{\mathcal{G}_1}(v) \supseteq \text{RR}_1 \supseteq \text{RR}_2 = \text{RR}_{\mathcal{G}_2}(v)$$

when $\Pr[e \in \mathcal{G}_{\text{IC}}] = \Pr[e \in \mathcal{G}_{\text{SIR}}]$ for any $e \in E$.

Proof. We first claim that $\text{RR}_2 = \text{RR}_{\mathcal{G}_2}(v)$. Since $\text{RR}_2 \subseteq \text{RR}_{\mathcal{G}_2}(v)$, it suffices to show $\text{RR}_{\mathcal{G}_2}(v) \setminus \text{RR}_2 = \emptyset$. Otherwise, for arbitrary $u \in \text{RR}_{\mathcal{G}_2}(v) \setminus \text{RR}_2$, there exists a directed path $P = (u_1 = u, u_2, \dots, u_\ell = v)$ in \mathcal{G}_2 . However, our coupling procedure would include each u_i ($i \in [\ell]$) in RR_2 contradicting $\text{RR}_{\mathcal{G}_2}(v) \setminus \text{RR}_2 \neq \emptyset$.

As for $\text{RR}_1 \supseteq \text{RR}_2$, it holds simply by the positive correlation property of SIR in Lemma 9 and the assumption $\Pr[e \in \mathcal{G}_{\text{IC}}] = \Pr[e \in \mathcal{G}_{\text{SIR}}]$ for any directed edge $e \in E$. Again, $\text{RR}_{\mathcal{G}_1}(v) \supseteq \text{RR}_1$ is obvious, and the proof is complete combining all these facts. \square

We are now ready to complete the proof of Lemma 11.

Proof of Lemma 11. As Lemma 12 shown, $(\mathcal{G}_1, \mathcal{G}_2)$ is the coupling of \mathcal{G}_{IC} and \mathcal{G}_{SIR} . Moreover, for any seed set $S \subseteq V$, $S \cap \text{RR}_{\text{SIR}}(v) \neq \emptyset$ implies $S \cap \text{RR}_{\text{IC}}(v) \neq \emptyset$ since $\text{RR}_{\mathcal{G}_1}(v)$ is the superset of $\text{RR}_{\mathcal{G}_2}(v)$ by Lemma 13. Hence, the inequality holds. \square

4.3 Significant Dominance

In the previous section, we have shown that, conditioned on the comparable spreading ability of each edge, there is a domination from IC to SIR. In this section, we demonstrate that such domination can be significant in some networks. This dominance further yields significantly different seeding strategies under these two models. The graph we construct is represented in Figure 1.

We show that for some specific social networks, the influence spread of IC could significantly dominate SIR with parameters satisfying Equation (1).

The following proposition shows that, for the instance in Figure 1, the influence spread of IC can significantly dominate that of SIR for the seed set $\{v\}$ if the parameters b , n_0 , β , and γ are set appropriately.

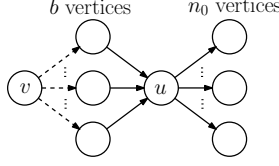


Figure 1: An instance to show the significant dominance. A vertex v is connected to b vertices by b dashed edges, and these b vertices are connected to a vertex u by b solid edges. Finally, u is connected to n_0 vertices by n_0 solid edges. The solid edges are “deterministic”, meaning that the parameters β and p in both IC and SIR models are set to 1. For the dashed edges, they share the same SIR parameters β and γ , and their IC parameter is decided based on β , γ and Equation (1). The values of b , n_0 , β , and γ are to be decided.

Proposition 14. *Consider the instance in Figure 1. For any $R > 0$, there exist b , n_0 , β , and γ such that $\frac{\sigma_{\text{IC}}(\{v\})}{\sigma_{\text{SIR}}(\{v\})} > R$.*

The high-level idea for Proposition 14 is as follows. By setting n_0 to be very large, $\sigma(\{v\})$ under both models is approximately proportional to the probability that vertex u is infected. It then remains to argue that u is infected with a significantly smaller probability in the SIR model. Notice that, by the definition of the solid edges, u is infected (with probability 1) once one of its in-neighbors is infected. Therefore, all we care about is the probability that *at least one of the b vertices is infected*, which is 1 minus the probability that none of the b vertices is infected. The latter probability is significantly higher in the SIR model due to the positive correlation in Lemma 9. The formal proof of Proposition 14 is available in Appendix A.

4.4 Difference in Seeding Strategies

We have shown that the expected number of infections under IC is weakly larger than that under SIR given the same seed set and with the matching parameters, and sometimes IC significantly dominates SIR. This significant dominance yields significant different seeding strategies under these two models, as shown by an example illustrated in Figure 2.

In Figure 2, the two red nodes are potential seeds. The red node on the left-hand side is the center of a star, while, on the right-hand side, we duplicate the gadget in Figure 1 such that the node v in Figure 1 is the red node (i.e., all the duplications share only the same vertex v ; two duplications are drawn in Figure 2). By Proposition 14, the seed on the right-hand side is much more powerful in the IC model than that in the SIR model; the seed on the left-hand side has the same power in both models. The reader can easily verify that, by appropriately setting up the parameters, the seed on the left-hand side is a much better choice for the SIR model and the seed on the right-hand side is a much better choice for the IC model.

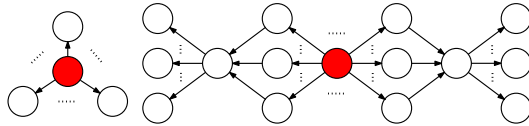


Figure 2: A graph to show the discrepancy of seeding strategy in IC and SIR.

5 InfMax in the SIR-based Models

In this section, we present algorithmic results for InfMax in the SIR model. It is worth noting that InfMax in various diffusion models can be formulated as a *submodular* optimization problem. In our case with the SIR model, the expected influence spread function $\sigma(\cdot)$ is also submodular. This follows from the fact that a diffusion model with a live-edge graph formulation is always submodular [Kempe et al., 2015]. With submodularity, it is well-known that the simple greedy algorithm achieves a $(1 - 1/e)$ -approximation [Nemhauser et al., 1978]. However, computing the function $\sigma(\cdot)$ is a #P-hard problem [Kempe et al., 2015, Chen et al.,

2010a,b]. To apply the greedy algorithm, the influence spread function $\sigma(\cdot)$ is approximated by the Monte-Carlo method, so we have a randomized algorithm that achieves a $(1 - 1/e - \epsilon)$ -approximation with high probability. Notice that this approximation ratio is optimal assuming $P \neq NP$, as InfMax is NP-hard to approximate to within a factor of more than $(1 - 1/e)$ for the IC model [Kempe et al., 2015], and the special case of the SIR model with $\gamma_u = 1$ for every $u \in V$ is exactly the IC model.

Despite that the greedy algorithms based on the Monte-Carlo are slow in practice. Researchers have then focused on designing algorithms that are fast in practice while keeping the theoretical approximation guarantee. One of the most successful types of such algorithms is based on *reverse-reachable sets* [Borgs et al., 2014, Tang et al., 2014, 2015, Chen, 2018], which yields a near-linear time algorithm with $1 - 1/e$ approximation ratio. The reverse reachable set technique, proposed by Borgs et al. [2014], makes use of the observation in Proposition 8. Our objective is to find S that maximizes $\Pr[S \cap \text{RR}_{\mathcal{G}} \neq \emptyset]$. This is done by sampling a sufficient number of copies of $\text{RR}_{\mathcal{G}}$ and finding S that intersects as many copies as possible, which becomes a classical k -max coverage problem. This type of algorithm has been widely used for the IC model and proved successful in terms of scalability.

Subsequent reverse-reachable-set-based algorithms aim to reduce the number of $\text{RR}_{\mathcal{G}}$ sets sampled while still keeping the approximation guarantee. Notably, the IMM algorithm proposed by Tang et al. [2015] uses a martingale method to estimate the number of reverse reachable sets.

Algorithm 2: The IMM algorithmic framework $\text{IMM}(G, k, \epsilon, \ell)$

Input: A directed graph $G = (V, E)$ where $|V| = n, |E| = m$ with live-edge diffusion model \mathcal{G} , the size of the seed set k and parameters ϵ, ℓ .

Output: The seed set S^* .

- 1 $\alpha \leftarrow \sqrt{\ell \cdot \log n + \log 2}, \beta \leftarrow \sqrt{(1 - 1/e) \cdot (\log \binom{n}{k} + \ell \cdot \log n + \log 2)}$ and $\gamma \leftarrow 4 + \log(8 \cdot \log n) / \log n$;
- 2 $\ell' \leftarrow \ell + \log 2 / \log n + \gamma$ and $\epsilon' \leftarrow \sqrt{2} \cdot \epsilon$;
- 3 $\lambda' \leftarrow \frac{(2 + \frac{2}{3}\epsilon') \cdot (\log \binom{n}{k} + \ell' \cdot \log n + \log \log_2 n) \cdot n}{\epsilon'^2}$ and $\lambda^* \leftarrow 2 \cdot n \cdot ((1 - 1/e) \cdot \alpha + \beta)^2 \cdot \epsilon^{-2}$;
- 4 Initialize a set $\mathcal{R} = \emptyset$ and an integer $\text{LB} = 1$;
- 5 **for** $i = 1$ **to** $\log_2 n - 1$ **do**
- 6 $x \leftarrow \frac{n}{2^i}$ and $\theta_i = \frac{\lambda'}{x}$;
- 7 **while** $|\mathcal{R}| \leq \theta_i$ **do**
- 8 $\text{RR} \leftarrow \text{RRSampling}(G, \mathcal{G});$ // sample a single $\text{RR}_{\mathcal{G}}$ set
- 9 $\mathcal{R} \leftarrow \mathcal{R} \cup \{\text{RR}\};$
- 10 $S_i \leftarrow \text{NodeSelection}(G, \mathcal{R}, k);$ // see Algorithm 3
- 11 **if** $n \cdot F_{\mathcal{R}}(S_i) \geq (1 + \epsilon') \cdot x$ **then**
- 12 $\text{LB} = n \cdot F_{\mathcal{R}}(S_i) / (1 + \epsilon');$
- 13 **break;**
- 14 $\theta = \lambda^* / \text{LB};$
- 15 **while** $|\mathcal{R}| \leq \theta$ **do**
- 16 $\text{RR} \leftarrow \text{RRSampling}(G, \mathcal{G});$ // sample a single $\text{RR}_{\mathcal{G}}$ set
- 17 $\mathcal{R} \leftarrow \mathcal{R} \cup \{\text{RR}\};$
- 18 $S^* \leftarrow \text{NodeSelection}(G, \mathcal{R}, k);$ // see Algorithm 3
- 19 **return** S^* .

Compared to the algorithm proposed by Borgs et al. [2014], the IMM algorithm leverages the advantages of optimizing the size of the reverse reachable set required for estimating the influence spread. The detailed implementation is shown in Algorithm 2.¹ In the algorithm, we use \mathcal{R} to collect all the sampled reverse reachable sets and use $F_{\mathcal{R}}(S)$ to denote the fraction of reverse reachable sets in \mathcal{R} covered by any seed set $S \subseteq V$. Here, the framework fits many live-edge graph diffusion models by replacing the reverse reachable set sampling subroutine $\text{RRSampling}(G, \mathcal{G})$.

¹An issue in the original IMM algorithm was later discovered by Chen [2018]. The algorithm we present here is based on the version after the correction in Chen [2018].

Algorithm 3: NodeSelection(G, \mathcal{R}, k)

Input: A directed graph $G = (V, E)$, a collection of RR set \mathcal{R} and the size of the seed set k .
Output: A seed set S^* .

- 1 Initialize $S^* \leftarrow \emptyset$;
- 2 **while** ($|S^*| < k$) **and** ($V \setminus S^* \neq \emptyset$) **do**
- 3 $v \leftarrow \operatorname{argmax}_{u \in V} F_{\mathcal{R}}(S^* \cup u) - F_{\mathcal{R}}(S^*)$;
- 4 $S^* \leftarrow S^* \cup \{v\}$;
- 5 **return** S^* .

Let $R \subseteq V$ be the vertices of a reverse reachable set. Let $w(R)$ be the number of edges of G incident to R . Examining the analysis of the IMM algorithm in Tang et al. [2015] and Chen [2018], one can verify the following lemma.

Lemma 15. *Consider a directed graph $G = (V, E)$ where $|V| = n, |E| = m$ with live-edge diffusion model \mathcal{G} , the size of the seed set k and parameters ε, ℓ . If the subroutine $\text{RRSampling}(G, \mathcal{G})$ returns an $\text{RR}_{\mathcal{G}}$ set R in $\alpha \cdot w(R)$ time, the algorithm $\text{IMM}(G, k, \varepsilon, \ell)$ (Algorithm 2) returns a $(1 - 1/e - \varepsilon)$ -approximate solution with at least $1 - 1/n^\ell$ probability in $O(\alpha \cdot (k + \ell)(m + n) \log n / \varepsilon^2)$ time.*

In the following, we introduce how we adapt the IMM algorithm to the SIR model and its variants TSIR. Specifically, we will design the subroutine RRSampling that is specifically for the SIR model and the TSIR model respectively.

5.1 Algorithm for InfMax with SIR Model

For the SIR model, one natural idea is to sample each RR_{SIR} based on the live-edge graph definition in Section 3.1.1. However, both \mathbf{R}_v and \mathbf{I}_e are sequences of infinitely many random variables. To accurately and efficiently sample a reverse reachable set RR_{SIR} , we instead directly calculate the probability that an edge is live. For example, $\Pr[e \in \mathcal{G}_{\text{SIR}}]$ can be computed by Equation (1), which is a geometric series that admits a compact formula. More generally, for a vertex u with a set E'_u of u 's incident edges and a particular incident edge e , the conditional probability $\Pr[e \in \mathcal{G}_{\text{SIR}} \mid E'_u \cap \mathcal{G}_{\text{SIR}} = \emptyset]$ can also be expressed as a geometric series by applying the law of conditional probability. With these, the reverse reachable set RR_{SIR} can be sampled in a way similar to the coupling procedure (Algorithm 1) in the proof of Lemma 11. Details for our algorithms are available in Algorithm 4. Based on the IMM algorithmic framework, we propose the SIRIMM method by extending the IMM algorithm to SIR, specifically, we designed the $\text{RR}_{\text{SIR}}\text{Sampling}(G, \beta, \gamma)$ that sample the reverse reachable set for SIR. The sampling algorithm can be easily adapted from the coupling process Algorithm 1. As mentioned in Section 5, we can directly compute the probability that an edge is live. Specifically, for each node u , let $\Gamma_u = \{v_1, \dots, v_\ell\}$ represent the set of outgoing neighbors of u in a fixed order. Denote by γ and β the recovery probability and infection probability in the SIR model, respectively. We compute the probability that u successfully infects its i -th neighbor, conditioned on u having failed to infect all of the first $i - 1$ neighbors, as follows:

$$\begin{aligned} & \Pr[v_i \mid \overline{v_{[i-1]}}] \\ &= \frac{\Pr[v_i \wedge \overline{v_{[i-1]}}]}{\Pr[\overline{v_{[i-1]}}]} \\ &= \frac{\sum_{t=1}^{\infty} (1 - \gamma)^{(t-1)} \cdot \gamma \cdot (1 - \beta)^{(i-1) \cdot t} (1 - (1 - \beta)^t)}{\sum_{t=1}^{\infty} (1 - \gamma)^{(t-1)} \cdot \gamma \cdot (1 - \beta)^{(i-1) \cdot t}} \\ &= \frac{\frac{(1 - \beta)^{(i-1)}}{1 - (1 - \gamma)(1 - \beta)^{(i-1)}} - \frac{(1 - \beta)^i}{1 - (1 - \gamma)(1 - \beta)^i}}{\frac{(1 - \beta)^{(i-1)}}{1 - (1 - \gamma)(1 - \beta)^{(i-1)}}} \end{aligned}$$

where $v_i \in \Gamma_u$ is the i -th neighbor of u , and $v_{[i-1]} \subseteq \Gamma_u$ represents the first $i - 1$ neighbors of u , and we slightly abuse the notations by letting v_i denote the event that u successfully infects v_i and $\overline{v_{[i-1]}}$ denote the event that u fails to infect each vertex in $v_{[i-1]}$.

Algorithm 4: $\text{RR}_{\text{SIR}}\text{Sampling}(G, \beta, \gamma)$

Input: A directed graph $G = (V, E)$ with the $\text{SIR}_{\beta, \gamma}$ diffusion model.

Output: A RR_{SIR} set.

```
1 Label an arbitrary order on the nodes and edges in  $G$ ;  
2 Sample a node  $v \in V$  uniformly at random;  
3 Initialize  $\text{RR}_{\text{SIR}} \leftarrow \{v\}$ , and  $E'_u \leftarrow \emptyset$  for any  $u \in V$ ;  
4 while  $A \leftarrow \{u \in V \setminus \text{RR}_{\text{SIR}} \mid \exists u' \in \text{RR}_{\text{SIR}}, (u, u') \in E \setminus E'_u\}$  and  $A \neq \emptyset$  do  
5   Select the node  $u \in A$  with the smallest index;  
6   Let  $((u, u_1), (u, u_2), \dots, (u, u_\ell))$  be the directed edges not in  $E'_u$  with endpoints in  $\text{RR}_{\text{SIR}}$  listed  
   by the index order;  
7    $j \leftarrow 0$ , flag  $\leftarrow 0$ ;  
8   repeat  
9      $j \leftarrow j + 1$ ;  
10    Sample  $p \sim \text{Unif}[0, 1]$ ;  
11     $\text{RR}_{\text{SIR}} \leftarrow \text{RR}_{\text{SIR}} \cup \{u\}$ , flag  $\leftarrow 1$  when  $p \leq \Pr[(u, u_j) \in \mathcal{G}_{\text{SIR}} \mid E'_u \cap \mathcal{G}_{\text{SIR}} = \emptyset]$ ;  
12     $E'_u \leftarrow E'_u \cup \{(u, u_j)\}$ ;  
13  until  $j = \ell$  or flag = 1;  
14 return  $\text{RR}_{\text{SIR}}$ .
```

Therefore, the probability $\Pr[v_i \mid \overline{v_{[i-1]}}]$ can be computed in $O(1)$ time. With this, the remaining details for sampling a reverse-reachable set are the same as they are in the IC model. Our algorithm is presented in Algorithm 4. According to Lemma 13, our algorithm returns RR_{SIR} faithfully.

Replacing the RR Sampling procedure in Algorithm 2 by Algorithm 4, we obtain the SIRIMM which returns an $(1 - 1/e - \epsilon)$ -approximate solution with at least probability $1 - 1/n^\ell$.

Since the (conditional) probability that an edge is live can be computed in $O(1)$ time, the time complexity for sampling a single reverse reachable set is the same as in the IC model, namely, $\alpha \cdot w(R)$ for $\alpha = O(1)$. By Lemma 15, the time complexity for SIRIMM is $O((k + \ell)(m + n) \log n/\epsilon^2)$.

Theorem 16. *There exists an algorithm that takes as inputs $k, \ell \in \mathbb{Z}^+$ and $\epsilon \in \mathbb{R}^+$, and a directed graph $G = (V, E)$ where $|V| = n, |E| = m$ with the diffusion model $\text{SIR}_{\beta, \gamma}$ and outputs a $(1 - 1/e - \epsilon)$ -approximately optimal expected influence spread of k seeds with at least $1 - 1/n^\ell$ probability in $O((k + \ell) \cdot (n + m) \cdot \log n/\epsilon^2)$ time.*

5.2 Algorithm for InfMax with TSIR Model

The case with the TSIR model is more involved due to the extra time-dependency. Intuitively, $\text{RR}_{\text{TSIR}}(v)$ is a truncated version of $\text{RR}_{\text{SIR}}(v)$. In addition, we need extra information in addition to the probability $\Pr[e = (u, v) \in \mathcal{G}_{\text{SIR}}]$, as it now matters in which round the infection across (u, v) succeeds. Therefore, we have to apply the original definition in Section 3.1.2 to sample a reverse reachable set. Due to the time-dependency feature, we need to truncate those vertices in $\text{RR}_{\text{SIR}}(v)$ that are too far away from v . This is done by applying Dijkstra's algorithm to maintain a reverse shortest path tree rooted at v . Notice that we do not need to consider infinitely many random variables for \mathbf{R}_v and \mathbf{I}_e : vertices that are not recovered or edges that are not active for long periods need not be considered due to the time-dependency of the TSIR model.

We design the approximation algorithm TSIRIMM for InfMax in the TSIR model by simulating the live-edge graph for the TSIR model to sample a reverse reachable set, as shown in Algorithm 5. The algorithm begins by selecting a node $v \in V$ uniformly at random, and v is added to the set RR_{TSIR} . Whenever a new node u is added to RR_{TSIR} , we explore all its incoming neighbors. Notice that those neighbors may have been explored before. For each in-neighbor w , if it has not been explored before, we sample its recovery time; otherwise, the recovery time for w has been sampled before, and we do nothing (Line 7-11). After this, we sample the number of rounds for the infection along the edge (u, w) to be successful (Line 14-22). If the number of rounds is more than the recovery time of w , the edge (u, w) is not included in the edge set

E_{TSIR} . Otherwise, we include (u, w) in E_{TSIR} , and let the said number of rounds be its *weight*. We now end up with a weighted graph (Line 25), where vertices that are reachable to v are those vertices that can infect v *without the time constraint* T . Finally, to impose the time constraint T , we find all vertices u whose distance to v is at most T (Line 26). This can be done by the standard Dijkstra’s algorithm.

Algorithm 5: $\text{RR}_{\text{TSIR}}\text{Sampling}(G, \beta, \gamma, T)$

Input: A directed graph $G = (V, E)$ with parameters β, γ and a time limit T .
Output: An RR_{TSIR} set.

- 1 Sample a node $v \in V$ uniformly at random;
- 2 Initialize $\text{RR}_{\text{TSIR}} \leftarrow \{v\}$, $E_{\text{TSIR}} \leftarrow \emptyset$, and $\text{RecRound}_u \leftarrow \perp$ for each $u \in V$;
- 3 Initialize $\text{ToBeProcessed} \leftarrow \{v\}$;
- 4 **while** $\text{ToBeProcessed} \neq \emptyset$ **do**
- 5 Get $u \in \text{ToBeProcessed}$ and remove u from ToBeProcessed ;
- 6 **for each in-neighbor** w **of** u **do**
- 7 $t \leftarrow 0$;
- 8 **while** $\text{RecRound}_w = \perp$ **and** $t \leq T$ **do**
- 9 $t \leftarrow t + 1$ and sample $p \sim \text{Unif}[0, 1]$;
- 10 set $\text{RecRound}_w \leftarrow t$ if $p \leq \gamma_w$;
- 11 **end**
- 12 $t \leftarrow 0$;
- 13 **repeat**
- 14 $t \leftarrow t + 1$ and sample $p \sim \text{Unif}[0, 1]$;
- 15 **if** $p \leq \beta_{w,u}$ **then**
- 16 update $\text{ToBeProcessed} \leftarrow \text{ToBeProcessed} \cup \{w\}$ if $w \notin \text{RR}_{\text{TSIR}}$;
- 17 $E_{\text{TSIR}} \leftarrow E_{\text{TSIR}} \cup \{(w, u)\}$;
- 18 $\text{RR}_{\text{TSIR}} \leftarrow \text{RR}_{\text{TSIR}} \cup \{w\}$;
- 19 $w_{w,u} \leftarrow t$;
- 20 **break**;
- 21 **end**
- 22 **until** $t > \text{RecRound}_w$ **or** $t > T$;
- 23 **end**
- 24 **end**
- 25 $G^* \leftarrow$ the edge-weighted graph $(\text{RR}_{\text{TSIR}}, E_{\text{TSIR}}, \{w_e\}_{e \in E_{\text{TSIR}}})$;
- 26 update $\text{RR}_{\text{TSIR}} \leftarrow \{u \in \text{RR}_{\text{TSIR}} \mid \text{the distance from } u \text{ to } v \text{ is at most } T \text{ in } G^*\}$;
- 27 **return** RR_{TSIR} .

Finally, to analyze the time complexity of Algorithm 5, notice that sampling the recovery time for each vertex and the number of rounds for which the infection along each edge (w, u) is successful requires $O(T)$ time, as we only need to flip the corresponding coin for at most T times. In addition, we need to perform Dijkstra’s algorithm at the end, which requires $O(|E_{\text{TSIR}}| + |\text{RR}_{\text{TSIR}}| \cdot \log(|\text{RR}_{\text{TSIR}}|))$ time, and we take the upper bound $O(w(R) \log(n))$. Therefore, the time complexity for sampling a reverse reachable set is $O(T \log(n) \cdot w(R))$. By Lemma 15, the overall time complexity for TSIRIMM is $O(T \cdot (k+l) \cdot (n+m) \cdot \log^2 n / \epsilon^2)$.

Theorem 17. *There exists an algorithm that takes as inputs $k, \ell, T \in \mathbb{Z}^+$ and $\epsilon \in \mathbb{R}^+$, and a directed graph $G = (V, E)$ where $|V| = n, |E| = m$ with the diffusion model $\text{TSIR}_{\beta, \gamma, T}$ and outputs a $(1 - 1/e - \epsilon)$ -approximate optimal expected influence spread of k seeds with at least $1 - 1/n^\ell$ probability in $O(T \cdot (k+l) \cdot (n+m) \cdot \log^2 n / \epsilon^2)$ time.*

6 Ablation Experiment

Our experiments consist of two parts. The first part compares the spreading influence of S under IC, SIR, and TSIR, with setting the parameter $p_{u,v}$ in IC and the infection rate $\beta_{u,v}$ and recover rate γ_v in SIR and

TSIR satisfying Equation (1):

$$p_{u,v} = \sum_{t=1}^{\infty} \gamma_u (1 - \gamma_u)^{t-1} (1 - (1 - \beta_{u,v})^t).$$

In the second part of our experiments, we compared the performance (including the seed qualities and the running times) of our proposed algorithm SIRIMM with four baseline methods, including CELF, IMM, DegDis, and the degree centrality algorithm, under the SIR model. The same experiments are performed for the TSIR model as well.

6.1 The Baseline Methods

The baseline methods we applied including IMM [Tang et al., 2015], CELF [Leskovec et al., 2007], DegDis [Chen et al., 2009], and, degree centrality algorithms [Freeman, 1978]. In this subsection, we will provide detailed descriptions of each baseline method. The details of IMM have already been described in Section 5.

6.1.1 The Degree Discount IC

The Degree Discount heuristic (DegDis) [Chen et al., 2009] is a popular algorithm used for identifying influential nodes in a network. The DegDis heuristic works by iteratively selecting the node with the highest degree and then removing it from the graph. This algorithm has been referred to as the “single degree discount heuristic” in previous literature, and we will adopt the name DegDis in this study. Another variant of this heuristic, known as “Degree Discount IC” (DegDis IC), was specifically designed by Chen et al. [Chen et al., 2012] for the *Uniform Independent Cascade model*, a special case of the IC model where the activation probability is the same for all edges.

In DegDis IC, the score of a candidate seed is computed by subtracting the number of its neighbors that have already been selected as seeds from its degree. This approach discounts the edges connecting the candidate seed to the existing seeds since they do not play a role in further infections. However, when considering the uniform independent cascade model, especially with a small parameter p , discounting by 1 can be inaccurate. To address this issue, the DegDis IC heuristic uses a more precise estimation of the Algorithm 6. For more details on this heuristic, readers can refer to reference [Chen et al., 2012].

Algorithm 6: DegreeDiscount (G, k)

Input: A directed graph $G = (V, E)$ with live-edge diffusion model \mathcal{G} , the number of spreaders k , and the parameter p .
Output: A set S including l influential nodes.

- 1 Initialize $S = \emptyset$;
- 2 **for** $v \in V$ **do**
- 3 $\text{dd}_v = d_v$; // d_v is the degree of v
- 4 Initialize $t_v = 0$;
- 5 **for** $i = 1$ **to** k **do**
- 6 Select $u = \arg \max_{v \in V} \{\text{dd}_v \mid v \in V \setminus S\}$;
- 7 $S = S \cup u$;
- 8 **for each neighbor** v **of** u **and** $v \in V \setminus S$ **do**
- 9 $t_v = t_v + 1$;
- 10 $\text{dd}_v = d_v - 2 \cdot t_v - (d_v - t_v) \cdot t_v \cdot p$;
- 11 **return** S ;

6.1.2 The Degree Centrality

The degree centrality method [Freeman, 1978] simply chooses k nodes with the largest degrees as the seeds.

6.1.3 CELF

CELF is an improved variant of the standard greedy algorithm that is 700 times faster [Leskovec et al., 2007]. In each iteration of the standard greedy algorithm, all nodes in the graph are tested and the node with the highest marginal influence is selected. In each iteration of CELF, by further exploiting submodularity of the cascade process, it identifies some nodes whose marginal influences are clearly sub-optimal and excludes these nodes from being tested. The core observation is that the marginal influence of each node in the current iteration will only be smaller than or equal to it is in the previous iteration. The algorithm’s details are shown in Algorithm 7.

Algorithm 7: CELF($G = (V, E), R, c, B, type$)

```

1  $\mathcal{A} \leftarrow \text{LazyForward}(G = (V, E), R, c, B, \text{UC});$ 
2  $\mathcal{A} \leftarrow \text{LazyForward}(G = (V, E), R, c, B, \text{CB});$ 
3 return  $R(\mathcal{A}_{\text{UC}}, \mathcal{A}_{\text{CB}})$ 

```

Algorithm 8: LazyForward($G = (V, E), R, c, B, type$)

```

1  $\mathcal{A} \leftarrow \emptyset;$ 
2 foreach  $s \in V$  do
3    $\delta_s \leftarrow +\infty;$ 
4   while  $\exists s \in V \setminus \mathcal{A} : c(\mathcal{A} \cup \{s\}) > 0$  do
5     foreach  $s \in V \setminus \mathcal{A}$  do
6        $cur_s \leftarrow \text{False};$ 
7       while True do
8         if  $type = \text{UC}$  then
9            $s^* \leftarrow \arg \max_{s \in V \setminus \mathcal{A}, c(\mathcal{A} \cup \{s\}) > 0} \delta_s;$ 
10          if  $type = \text{CB}$  then
11             $s^* \leftarrow \arg \max_{s \in V \setminus \mathcal{A}, c(\mathcal{A} \cup \{s\}) > 0} \delta_s / c(s);$ 
12          if  $cur_s$  then
13             $\mathcal{A} \leftarrow \mathcal{A} \cup s^*;$ 
14            Break;
15          else
16             $\delta_s \leftarrow R(\mathcal{A} \cup \{s\}) - R(\mathcal{A});$ 
17             $cur_s \leftarrow \text{True};$ 
18 return  $\mathcal{A};$ 

```

6.2 Results

All experiments are implemented in C++ and conducted on an Ubuntu 18.04.4 machine with Intel(R) Xeon(R) Gold 6240C CPU @2.60GHz and 251 GB RAM. We conducted the three sets of experiments on four real-world networks whose statistics are presented in Table 1.

6.2.1 Comparing the spreads of IC, SIR, and TSIR

In this section, we validate that in the graph G , given the same seeds S (S is obtained by IMM algorithm with $\epsilon = 0.5$ and $\ell = 1$), the influence spread of S in IC dominates its counterpart in SIR under corresponding parameters satisfied Equation (1). Here, we set $p \in \{0.01, 0.05, 0.1, 0.3, 0.5\}$ for IC, the recovery rate is set to 0.8 in SIR and TSIR, and the infected rate is calculated according to Equation (1). Specifically, the influence spread of S is measured by the number of nodes that end up in the *active* state in IC, and the

Table 1: The basic structural characteristics of the 4 networks. Here, N and M are the numbers of nodes and edges, respectively.

Network	N	M	Average Degree	Maximum Degree
CA-GrQc	5,242	14,490	5.53	81
DBLP	317081	1,049,866	6.62	306
Nethept	15,233	31,387	4.12	64
com-YouTube	1,134,890	2,987,624	5.26	28576

number of nodes that end up in the *recovered* states in SIR after the propagation process. For TSIR, T is set to $T = 100$. For a given seed set, the expected spread is measured by 10000 times of Monte-Carlo simulations. The only exception is that of com-YouTube where we set the number of Monte Carlo as 1000, due to the graph’s large scale.

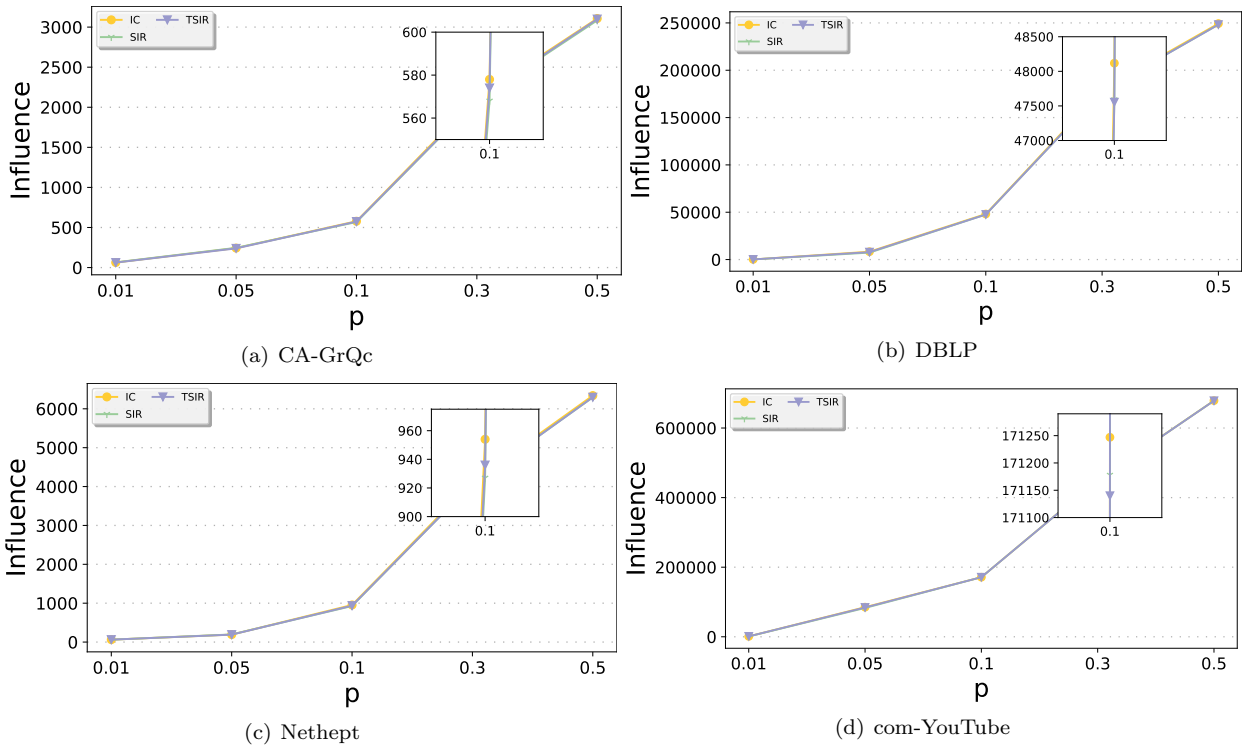


Figure 3: The performances of the same S under IC and SIR, with a set of matching parameters p , β and γ , respectively. Due to the significant overall fluctuations in the data, we use an inset plot to highlight the changes within a specific range. Without loss of generality, we show the specific fluctuation of Influence on the point when $p = 0.1$.

Figure 3 demonstrates the influence spread of S under IC, SIR, and TSIR across the different values of p . As expected, the result shows that the influence of S on IC dominates SIR and TSIR in real-world datasets, but by not a very large margin in general. As analyzed in Section 4, the positive correlation in SIR is the key factor causing this dominance. It is evident that in networks with dense edges, such as DBLP, this dominance is pronounced due to the significant impact of positive correlation in the SIR model.

6.2.2 Comparison of Algorithms by Seeds Qualities

In this section, we compare our proposed algorithms SIRIMM and TSIRIMM with the four baseline algorithms CELF, DegDis, IMM (by treating the SIR/TSIR diffusion model as the IC model according to Equation (1)),

and degree centrality. For the diffusion model parameters, we set $p = 0.1$, $\gamma = 0.8$, and β is calculated according to Equation (1). The parameters we used for these algorithms are shown in Table 2.

Table 2: Parameters for baseline approach.

Algorithms	Parameter	Value
CELFF	MC Simulations	10000
Degree Discount	p	0.1
IMM	ϵ	0.5
	ℓ	1
SIRIMM	ϵ	0.5
	ℓ	1
TSIRIMM	ϵ	0.5
	ℓ	1

We proceed to evaluate their performance by benchmarking their qualities. In our specific problem, quality refers to the expected spread generated by the k influential seeds identified by each algorithm, and the expected spread is measured by 10000 times of Monte-Carlo simulations. The only exception is that of com-YouTube where we set the number of Monte Carlo as 1000, due to the graph’s large scale.

Compare SIRIMM with baselines. Here we focus on the performance of seed in the SIR model by algorithms includes SIRIMM, DegDis, IMM, degree centrality, and CELF.

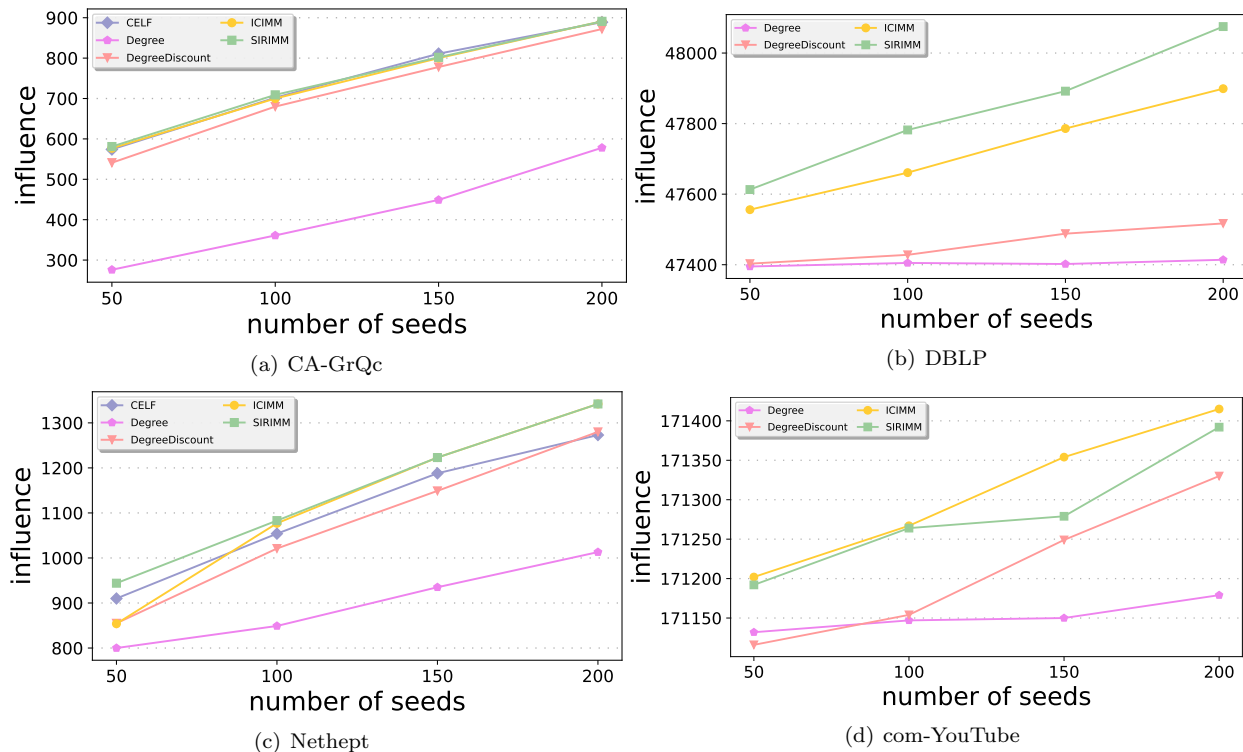


Figure 4: Comparing the influence spread of SIRIMM with baseline methods.

As shown in Figure 4, the influence spread of SIRIMM is higher than that of the baseline method in most cases. Although CELF and IMM are designed to greedily select the influential seeds, both of them are assumed based on the IC model, specifically, both of them try to approximate the result of SIR based on the IC model. Conversely, SIRIMM is designated tailored to the SIR model; naturally, the performance of SIRIMM is higher than its counterpart of CELF and IMM. Notice that, this difference is slight, the reason is akin to

the analysis in Section 6.2.1. As for DegDis and degree centrality, both of them are proposed to select seeds in a general way and have strong scalability, but failed to target on specific diffusion models.

Compare TSIRIMM with baselines. Here we focus on the performance of seed selection in the TSIR model by algorithms including DegDis, IMM, degree centrality, and CELF.

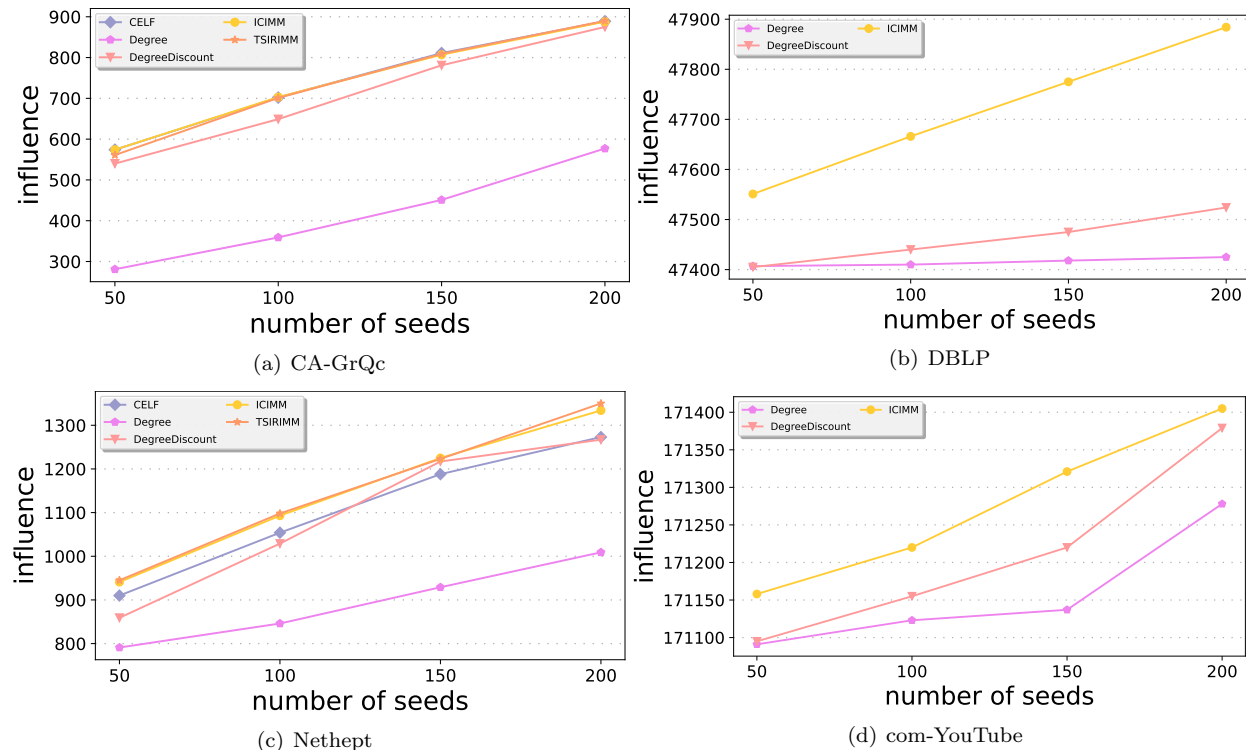


Figure 5: Comparing the influence spread of TSIRIMM with baseline methods.

As shown in Figure 5, the influence spread of TSIRIMM is higher than that of the baseline method in CA-GrQc and Nethept based on the TSIR model, which is because TSIRIMM is specifically designed based on TSIR model while the others are not. However, due to the extra complications of computing shortest paths in the RR set sampling process (caused by the time-dependency feature of the TSIR model), TSIRIMM has a much lower scalability. In particular, it fails to scale to DBLP and com-YouTube (the algorithm did not terminate after more than 48 hours). The algorithm CELF also fails to scale to DBLP and com-YouTube as the Monte-Carlo sampling used by CELF is generally slower than RR sets sampling.

6.2.3 Comparison of Algorithms by Running Times

In this analysis, we investigate the running time of our algorithms (SIRIMM and TSIRIMM), greedy method CELF, DegDis, IMM, and degree centrality. The parameter T for the TSIR model (and thus the algorithm TSIRIMM) is set to $T = 50$.

As shown in Figure 6, the running time of our proposed TSIRIMM and SIRIMM and the baseline methods are compared. As mentioned before, the running times of TSIRIMM and CELF on DBLP and com-YouTube are missing.

In CA-GrQc and Nethept, the running time of CELF is significantly higher than that of the other methods (IMM, SIRIMM, DegDis, and degree centrality). As expected, TSIRIMM also has a higher running time than the other methods. However, the gap between TSIRIMM and the other methods is smaller than the gap between CELF and the other methods. In DBLP and com-YouTube, the running time of SIRIMM is slightly higher than the remaining baselines, which is because of the RR set sampling process in the SIRIMM method.

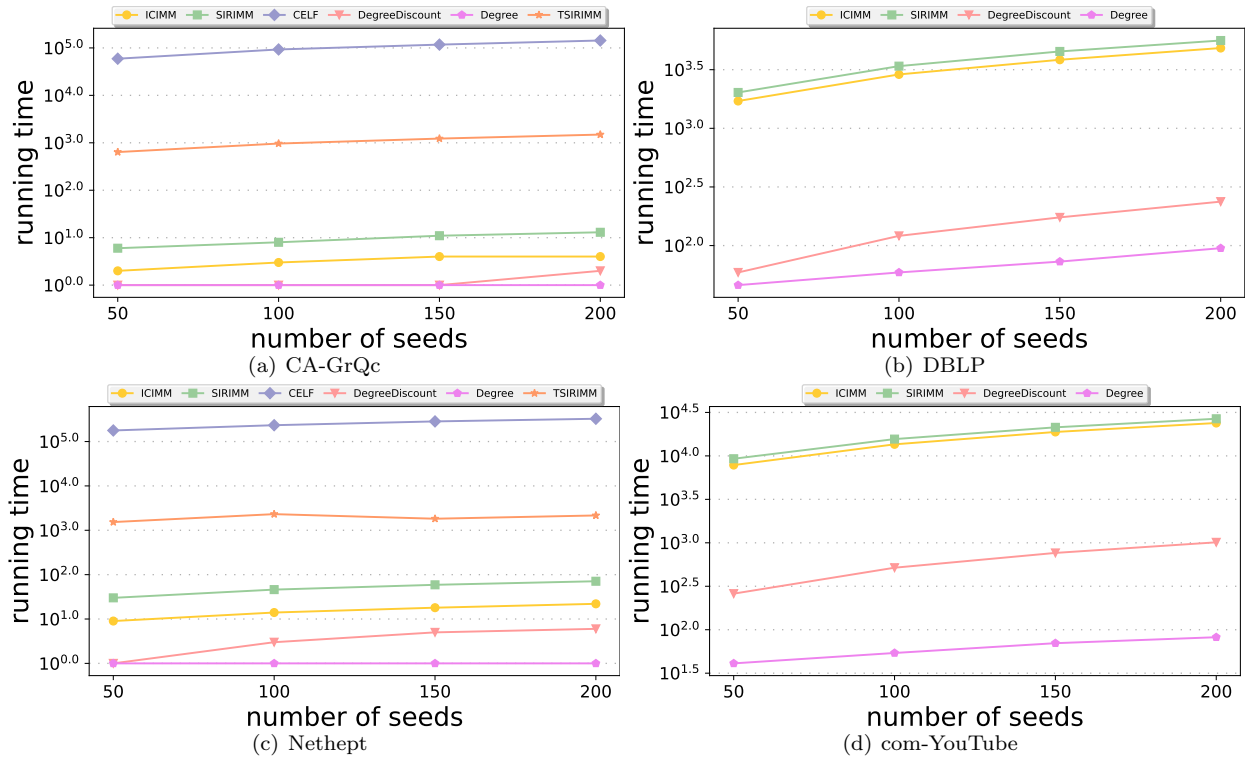


Figure 6: Comparing the scalability of SIRIMM, TSIRIMM with greedy and heuristics.

7 Conclusion

In this paper, we have explored the similarities and differences between the two diffusion models: IC and SIR. Prior work has observed that the SIR model can be “approximately” viewed by the IC model when the IC parameter of each edge (u, v) is viewed as an aggregated probability that u eventually infects v in the SIR model (see Equation (1)). However, if viewed in this way, there is a dependency on the outgoing edges of every vertex in the SIR model. In this paper, we have performed an in-deep analysis on this dependency both theoretically and empirically. We have proved that this extra dependency always harms the spread of influence. As a result, under matching parameters, given the same seed set, the influence spread under the IC model dominates that under the SIR model. We have also shown that this domination can be significant in the theoretical worst-case analysis, while it is less significant in our empirical experiments.

By exploiting some of our proof techniques, we adapt the IMM algorithm to the InfMax problem under the SIR diffusion model and the TSIR model (which is a time-dependent variant of the SIR model). To the best of our knowledge, this is the first InfMax algorithm for the SIR model with the $(1 - 1/e)$ theoretical guarantee.

Acknowledgments

The research of Biaoshuai Tao was supported by the National Natural Science Foundation of China (No. 62102252). The research of Kuan Yang was supported by the NSFC grant No. 62102253.

References

- Linda J.S. Allen. Some discrete-time SI, SIR, and SIS epidemic models. *Mathematical Biosciences*, 124(1):83–105, 1994. ISSN 0025-5564. doi: [https://doi.org/10.1016/0025-5564\(94\)90025-6](https://doi.org/10.1016/0025-5564(94)90025-6). URL <https://www.sciencedirect.com/science/article/pii/0025556494900256>. 2

- Rico Angell and Grant Schoenebeck. Don't be greedy: Leveraging community structure to find high quality seed sets for influence maximization. In *Web and Internet Economics: 13th International Conference, WINE 2017, Bangalore, India, December 17–20, 2017, Proceedings 13*, pages 16–29. Springer, 2017. [4](#)
- Frank M. Bass. *A New Product Growth Model for Consumer Durables*, pages 351–353. Springer Berlin Heidelberg, Berlin, Heidelberg, 1976. ISBN 978-3-642-51565-1. doi: 10.1007/978-3-642-51565-1_107. URL https://doi.org/10.1007/978-3-642-51565-1_107. [2](#)
- Christian Borgs, Michael Brautbar, Jennifer Chayes, and Brendan Lucier. Maximizing social influence in nearly optimal time. In *Proceedings of the twenty-fifth annual ACM-SIAM symposium on Discrete algorithms*, pages 946–957. SIAM, 2014. [3](#), [4](#), [6](#), [8](#), [14](#)
- Jacqueline Johnson Brown and Peter H. Reingen. Social Ties and Word-of-Mouth Referral Behavior*. *Journal of Consumer Research*, 14(3):350–362, 12 1987. ISSN 0093-5301. doi: 10.1086/209118. URL <https://doi.org/10.1086/209118>. [1](#), [2](#)
- Carmen Camarero and Rebeca San José. Social and attitudinal determinants of viral marketing dynamics. *Computers in Human Behavior*, 27(6):2292–2300, 2011. ISSN 0747-5632. doi: <https://doi.org/10.1016/j.chb.2011.07.008>. URL <https://www.sciencedirect.com/science/article/pii/S0747563211001464>. [2](#)
- Ning Chen. On the approximability of influence in social networks. *SIAM Journal on Discrete Mathematics*, 23(3):1400–1415, 2009. [4](#)
- Wei Chen. An issue in the martingale analysis of the influence maximization algorithm imm. In *Computational Data and Social Networks: 7th International Conference, CSoNet 2018, Shanghai, China, December 18–20, 2018, Proceedings 7*, pages 286–297. Springer, 2018. [3](#), [14](#), [15](#)
- Wei Chen. Network diffusion models and algorithms for big data. *POSTS & TELECOM PRESS, Bei Jing*, 2020. [2](#)
- Wei Chen and Binghui Peng. On adaptivity gaps of influence maximization under the independent cascade model with full adoption feedback. *arXiv preprint arXiv:1907.01707*, 2019. [4](#)
- Wei Chen, Yajun Wang, and Siyu Yang. Efficient influence maximization in social networks. In *Proceedings of the 15th ACM SIGKDD International Conference on Knowledge Discovery and Data Mining, KDD '09*, page 199–208, New York, NY, USA, 2009. Association for Computing Machinery. ISBN 9781605584959. doi: 10.1145/1557019.1557047. URL <https://doi.org/10.1145/1557019.1557047>. [4](#), [18](#)
- Wei Chen, Chi Wang, and Yajun Wang. Scalable influence maximization for prevalent viral marketing in large-scale social networks. In *Proceedings of the 16th ACM SIGKDD international conference on Knowledge discovery and data mining*, pages 1029–1038, 2010a. [13](#)
- Wei Chen, Yifei Yuan, and Li Zhang. Scalable influence maximization in social networks under the linear threshold model. In *2010 IEEE international conference on data mining*, pages 88–97. IEEE, 2010b. [14](#)
- Wei Chen, Carlos Castillo, and Laks VS Lakshmanan. *Information and influence propagation in social networks*. Springer Nature, 2022a. [2](#)
- Wei Chen, Binghui Peng, Grant Schoenebeck, and Biaoshuai Tao. Adaptive greedy versus non-adaptive greedy for influence maximization. *Journal of Artificial Intelligence Research*, 74:303–351, 2022b. [4](#)
- Yi-Cheng Chen, Wen-Chih Peng, and Suh-Yin Lee. Efficient algorithms for influence maximization in social networks. *Knowledge and Information Systems*, 33:577–601, 12 2012. ISSN 0219-1377. doi: 10.1007/s10115-012-0540-7. [3](#), [4](#), [18](#)
- Gianlorenzo D'Angelo, Debashmita Poddar, and Cosimo Vinci. Improved approximation factor for adaptive influence maximization via simple greedy strategies. *arXiv preprint arXiv:2007.09065*, 2020. [4](#)

- Gianlorenzo D'Angelo, Debashmita Poddar, and Cosimo Vinci. Better bounds on the adaptivity gap of influence maximization under full-adoption feedback. *Artificial Intelligence*, 318:103895, 2023. 4
- Pedro Domingos and Matt Richardson. Mining the network value of customers. In *Proceedings of the Seventh ACM SIGKDD International Conference on Knowledge Discovery and Data Mining*, KDD '01, page 57–66, New York, NY, USA, 2001. Association for Computing Machinery. ISBN 158113391X. doi: 10.1145/502512.502525. URL <https://doi.org/10.1145/502512.502525>. 1, 2
- Matthias Ehrhardt, Ján Gašper, and Soňa Kilianová. SIR-based mathematical modeling of infectious diseases with vaccination and waning immunity. *Journal of Computational Science*, 37:101027, 2019. 3
- Linton C. Freeman. Centrality in social networks conceptual clarification. *Social Networks*, 1(3):215–239, 1978. ISSN 0378-8733. doi: [https://doi.org/10.1016/0378-8733\(78\)90021-7](https://doi.org/10.1016/0378-8733(78)90021-7). URL <https://www.sciencedirect.com/science/article/pii/0378873378900217>. 4, 18
- Amit Goyal, Wei Lu, and Laks VS Lakshmanan. Celf++ optimizing the greedy algorithm for influence maximization in social networks. In *Proceedings of the 20th international conference companion on World wide web*, pages 47–48, 2011. 3, 4
- Priscilla E Greenwood and Luis F Gordillo. Stochastic epidemic modeling. *Mathematical and statistical estimation approaches in epidemiology*, pages 31–52, 2009. 2
- KM Ariful Kabir, Kazuki Kuga, and Jun Tanimoto. Analysis of SIR epidemic model with information spreading of awareness. *Chaos, Solitons & Fractals*, 119:118–125, 2019. 3
- David Kempe, Jon M. Kleinberg, and Éva Tardos. Maximizing the spread of influence through a social network. *Theory Comput.*, 11:105–147, 2015. 1, 2, 3, 4, 5, 6, 13, 14
- William Ogilvy Kermack and Anderson G McKendrick. A contribution to the mathematical theory of epidemics. *Proceedings of the royal society of london. Series A, Containing papers of a mathematical and physical character*, 115(772):700–721, 1927. 2, 5
- Sanjeev Khanna and Brendan Lucier. Influence maximization in undirected networks. In *Proceedings of the twenty-fifth annual ACM-SIAM symposium on Discrete algorithms*, pages 1482–1496. SIAM, 2014. 4
- Fang Kong, Jize Xie, Baoxiang Wang, Tao Yao, and Shuai Li. Online influence maximization under decreasing cascade model, 2023. 4
- Sunil Kumar, Ali Ahmadian, Ranbir Kumar, Devendra Kumar, Jagdev Singh, Dumitru Baleanu, and Mehdi Salimi. An efficient numerical method for fractional SIR epidemic model of infectious disease by using bernstein wavelets. *Mathematics*, 8(4):558, 2020. 3
- Theodoros Lappas, Kun Liu, and Evimaria Terzi. A survey of algorithms and systems for expert location in social networks. *Social network data analytics*, pages 215–241, 2011. 2
- Kristina Lerman and Rumi Ghosh. Information contagion: An empirical study of the spread of news on digg and twitter social networks. *Proceedings of the International AAAI Conference on Web and Social Media*, 4(1):90–97, May 2010. doi: 10.1609/icwsm.v4i1.14021. URL <https://ojs.aaai.org/index.php/ICWSM/article/view/14021>. 1
- Jure Leskovec, Andreas Krause, Carlos Guestrin, Christos Faloutsos, Jeanne VanBriesen, and Natalie Glance. Cost-effective outbreak detection in networks. In *Proceedings of the 13th ACM SIGKDD international conference on Knowledge discovery and data mining*, pages 420–429, 2007. 3, 4, 18, 19
- Longjie Li, Yanhong Wen, Shenshen Bai, and Panfeng Liu. Link prediction in weighted networks via motif predictor. *Knowledge-Based Systems*, 242:108402, 2022. 4
- Shuai Li, Fang Kong, Kejie Tang, Qizhi Li, and Wei Chen. Online influence maximization under linear threshold model, 2021. 4

- Yuchen Li, Ju Fan, Yanhao Wang, and Kian-Lee Tan. Influence maximization on social graphs: A survey. *IEEE Trans. on Knowledge and Data Engineering*, 30(10):1852–1872, 2018. 2
- Panfeng Liu, Longjie Li, Shiyu Fang, and Yukai Yao. Identifying influential nodes in social networks: A voting approach. *Chaos, Solitons & Fractals*, 152:111309, 2021. ISSN 0960-0779. doi: <https://doi.org/10.1016/j.chaos.2021.111309>. URL <https://www.sciencedirect.com/science/article/pii/S0960077921006639>. 4
- Panfeng Liu, Longjie Li, Yanhong Wen, and Shiyu Fang. Identifying influential nodes in social networks: Exploiting self-voting mechanism. *Big data*, 11(4):296–306, August 2023. ISSN 2167-6461. doi: 10.1089/big.2022.0165. 2
- Yuhua Long and Lin Wang. Global dynamics of a delayed two-patch discrete SIR disease model. *Communications in Nonlinear Science and Numerical Simulation*, 83:105117, 2020. 3
- Lijia Ma, Zengyang Shao, Xiaocong Li, Qiuzhen Lin, Jianqiang Li, Victor CM Leung, and Asoke K Nandi. Influence maximization in complex networks by using evolutionary deep reinforcement learning. *IEEE Transactions on Emerging Topics in Computational Intelligence*, 2022. 4
- Vijay Mahajan, Eitan Muller, and Frank M. Bass. New product diffusion models in marketing: A review and directions for research. *Journal of Marketing*, 54(1):1–26, 1990. doi: 10.1177/002224299005400101. URL <https://doi.org/10.1177/002224299005400101>. 2
- Elchanan Mossel and Sebastien Roch. Submodularity of influence in social networks: From local to global. *SIAM Journal on Computing*, 39:2176–2188, 1 2010. ISSN 0097-5397. doi: 10.1137/080714452. 4
- George L Nemhauser, Laurence A Wolsey, and Marshall L Fisher. An analysis of approximations for maximizing submodular set functions—i. *Mathematical programming*, 14:265–294, 1978. 4, 13
- Romualdo Pastor-Satorras and Alessandro Vespignani. Epidemic dynamics and endemic states in complex networks. *Physical Review E*, 63(6):066117, 2001. 1
- Binghui Peng and Wei Chen. Adaptive influence maximization with myopic feedback. *Advances in Neural Information Processing Systems*, 32, 2019. 4
- Matthew Richardson and Pedro Domingos. Mining knowledge-sharing sites for viral marketing. In *Proceedings of the eighth ACM SIGKDD international conference on Knowledge discovery and data mining*, pages 61–70, 2002. 1, 2
- Roberto Rigobon. Contagion: How to Measure It? In *Preventing Currency Crises in Emerging Markets*, NBER Chapters, pages 269–334. National Bureau of Economic Research, Inc, 2002. URL <https://ideas.repec.org/h/nbr/nberch/10638.html>. 1
- Gert Sabidussi. The centrality index of a graph. *Psychometrika*, 31:581–603, 12 1966. ISSN 0033-3123. doi: 10.1007/BF02289527. 4
- Grant Schoenebeck and Biaoshuai Tao. Beyond worst-case (in) approximability of nonsubmodular influence maximization. *ACM Transactions on Computation Theory (TOCT)*, 11(3):1–56, 2019. 4
- Grant Schoenebeck and Biaoshuai Tao. Influence maximization on undirected graphs: Toward closing the $(1-1/e)$ gap. *ACM Transactions on Economics and Computation (TEAC)*, 8(4):1–36, 2020. 4
- Grant Schoenebeck, Biaoshuai Tao, and Fang-Yi Yu. Limitations of greed: Influence maximization in undirected networks re-visited. *arXiv preprint arXiv:2002.11679*, 2020. 4
- Grant Schoenebeck, Biaoshuai Tao, and Fang-Yi Yu. Think globally, act locally: On the optimal seeding for nonsubmodular influence maximization. *Information and Computation*, 285:104919, 2022. 4
- Ndolane Sene. SIR epidemic model with mittag-leffler fractional derivative. *Chaos, Solitons & Fractals*, 137: 109833, 2020. 3

- Youze Tang, Xiaokui Xiao, and Yanchen Shi. Influence maximization: Near-optimal time complexity meets practical efficiency. In *Proceedings of the 2014 ACM SIGMOD International Conference on Management of Data*, SIGMOD '14, page 75–86, New York, NY, USA, 2014. Association for Computing Machinery. ISBN 9781450323765. doi: 10.1145/2588555.2593670. URL <https://doi.org/10.1145/2588555.2593670>. 3, 4, 14
- Youze Tang, Yanchen Shi, and Xiaokui Xiao. Influence maximization in near-linear time: A martingale approach. In *ACM SIGMOD Conference*, pages 1539–1554, 2015. 3, 4, 14, 15, 18
- Peng Wu and Li Pan. Scalable influence blocking maximization in social networks under competitive independent cascade models. *Computer Networks*, 123:38–50, 2017. ISSN 1389-1286. doi: <https://doi.org/10.1016/j.comnet.2017.05.004>. URL <https://www.sciencedirect.com/science/article/pii/S1389128617301962>. 2
- Qingyun Wu, Zhige Li, Huazheng Wang, Wei Chen, and Hongning Wang. Factorization bandits for online influence maximization. In *Proceedings of the 25th ACM SIGKDD International Conference on Knowledge Discovery & Data Mining*, KDD '19, page 636–646, New York, NY, USA, 2019. Association for Computing Machinery. ISBN 9781450362016. doi: 10.1145/3292500.3330874. URL <https://doi.org/10.1145/3292500.3330874>. 4
- Xiu-Xiu Zhan, Chuang Liu, Gui-Quan Sun, and Zi-Ke Zhang. Epidemic dynamics on information-driven adaptive networks. *Chaos, Solitons & Fractals*, 108:196–204, 2018. ISSN 0960-0779. doi: <https://doi.org/10.1016/j.chaos.2018.02.010>. URL <https://www.sciencedirect.com/science/article/pii/S0960077918300560>. 2

A Omitted Proofs

Proposition 4. \mathcal{G}_{SIR} defined above is a live-edge graph formulation of $\text{SIR}_{\beta,\gamma}$, namely,

$$\sigma_{\text{SIR}}(S) = \mathbf{E}[\text{the number of reachable nodes from } S \text{ in } \mathcal{G}_{\text{SIR}}].$$

Proof. The proof is just the rephrase of the stochastic diffusion process. We drive the diffusion process by the collection of random variables $\{\mathbf{R}_v\}_{v \in V}, \{\mathbf{I}_e\}_{e \in E}$ that generate the live-edge graph as mentioned in Section 3.1.1.

The diffusion process can be driven by $\{\mathbf{R}_v\}_{v \in V}, \{\mathbf{I}_e\}_{e \in E}$ as follows. Initially, each node $v \in V$ maintains an index $j_v = 1$, and the nodes in the seed set S are labeled as infected at timestamp 0. At each timestamp $t = 1, 2, \dots$, each infected node u from the previous timestamp $t - 1$ performs the following operations sequentially:

- for each of its susceptible outgoing neighbors v , u infects v if $I_{(u,v),j_u} = 1$;
- u gets recovered if $R_{u,j_u} = 1$ and remains infected otherwise;
- $j_u \leftarrow j_u + 1$.

Examining the randomness for any infected node u in the above process, one can verify that there exists a path in \mathcal{G}_{SIR} from S to u . Conversely, regarding the randomness for any path from S to the node u in \mathcal{G}_{SIR} , we can recover the diffusion process in which u gets infected. \square

Lemma 9. Given a directed graph $G = (V, E)$ with the diffusion model $\text{SIR}_{\beta,\gamma}$, we have

$$\Pr[e \in \mathcal{G}_{\text{SIR}} \mid E' \cap \mathcal{G}_{\text{SIR}} = \emptyset] \leq \Pr[e \in \mathcal{G}_{\text{SIR}}]$$

for any $E' \subseteq E$ and $e \in E \setminus E'$.

Proof. Suppose that e is an outgoing edge of u in the underlying graph G , and let E'_u be the collection of outgoing edges of a node u in the set E' . If $E'_u = \emptyset$, then by definition we have

$$\Pr[e \in \mathcal{G}_{\text{SIR}} \mid E' \cap \mathcal{G}_{\text{SIR}} = \emptyset] = \Pr[e \in \mathcal{G}_{\text{SIR}}].$$

Therefore, it suffices to consider the case when $E'_u \neq \emptyset$. Note that

$$\Pr[e \in \mathcal{G}_{\text{SIR}} \mid E' \cap \mathcal{G}_{\text{SIR}} = \emptyset] = \Pr[e \in \mathcal{G}_{\text{SIR}} \mid E'_u \cap \mathcal{G}_{\text{SIR}} = \emptyset] = \frac{\Pr[e \in \mathcal{G}_{\text{SIR}}, E'_u \cap \mathcal{G}_{\text{SIR}} = \emptyset]}{\Pr[E'_u \cap \mathcal{G}_{\text{SIR}} = \emptyset]}.$$

In the following, we prove

$$\Pr[e \in \mathcal{G}_{\text{SIR}}, E'_u \cap \mathcal{G}_{\text{SIR}} = \emptyset] \leq \Pr[e \in \mathcal{G}_{\text{SIR}}] \cdot \Pr[E'_u \cap \mathcal{G}_{\text{SIR}} = \emptyset] \quad (2)$$

by the coupling argument, which implies Lemma 9 immediately. Specifically, we introduce a unified probability space and demonstrate that the aforementioned terms are equivalent to the probability of specific events that can be defined in this space.

Let $\{\mathbf{R}_v\}_{v \in V}, \{\mathbf{R}'_v\}_{v \in V}$ and $\{\mathbf{I}_f\}_{f \in E}$ be collections of independent random variables as mentioned in Section 3. We define the graphs \mathcal{G}_1 and \mathcal{G}_2 as:

$$\mathcal{G}_1 := \mathcal{G}_{\text{SIR}}(\{\mathbf{R}_v\}_{v \in V}, \{\mathbf{I}_f\}_{f \in E}), \quad \mathcal{G}_2 := \mathcal{G}_{\text{SIR}}(\{\mathbf{R}'_v\}_{v \in V}, \{\mathbf{I}_f\}_{f \in E}).$$

We can then observe that Equation (2) is equivalent to

$$\Pr[e \in \mathcal{G}_1, E'_u \cap \mathcal{G}_1 = \emptyset] \leq \Pr[e \in \mathcal{G}_1, E'_u \cap \mathcal{G}_2 = \emptyset],$$

since the events $\{e \in \mathcal{G}_1\}$ and $\{E'_u \cap \mathcal{G}_2 = \emptyset\}$ are independent.

For each edge $f \in E$, let T_f be the first time that $I_{f,T_f} = 1$, i.e., $I_{f,T_f} = 1$ and $I_{f,[T_f-1]}$ is a sequence of 0 with length $T_f - 1$. We also call T_f as the infection time of edge $f \in E$. The event $\{e \in \mathcal{G}_1, E'_u \cap \mathcal{G}_1 = \emptyset\}$

happens only if the infection time of e is earlier than the infection time of any other edges in E'_u , i.e., $T_e < T_f$ for any $f \in E'_u$. For simplicity, let

$$\mathcal{E}_1 := \{e \in \mathcal{G}_1, E'_u \cap \mathcal{G}_1 = \emptyset, T_e < T_f, \forall f \in E'_u\},$$

and

$$\mathcal{E}_2 := \{e \in \mathcal{G}_1, E'_u \cap \mathcal{G}_2 = \emptyset, T_e < T_f, \forall f \in E'_u\}.$$

Observe that

$$\Pr[e \in \mathcal{G}_1, E'_u \cap \mathcal{G}_1 = \emptyset] = \Pr[\mathcal{E}_1], \quad \Pr[\mathcal{E}_2] \leq \Pr[e \in \mathcal{G}_1, E'_u \cap \mathcal{G}_2 = \emptyset].$$

Let $T^* := \min_{f \in E'_u} T_f$ and

$$P_1(t_1, t_2) := \Pr[e \in \mathcal{G}_1, E'_u \cap \mathcal{G}_1 = \emptyset, T_e = t_1, T^* = t_2],$$

$$P_2(t_1, t_2) := \Pr[e \in \mathcal{G}_1, E'_u \cap \mathcal{G}_2 = \emptyset, T_e = t_1, T^* = t_2],$$

for any positive integer $1 \leq t_1 < t_2$. It boils down to show $P_1(t_1, t_2) \leq P_2(t_1, t_2)$ since

$$\Pr[\mathcal{E}_1] = \sum_{t_1=1}^{\infty} \sum_{t_2=t_1+1}^{\infty} P_1(t_1, t_2) \quad \text{and} \quad \Pr[\mathcal{E}_2] = \sum_{t_1=1}^{\infty} \sum_{t_2=t_1+1}^{\infty} P_2(t_1, t_2).$$

By definition, we have

$$P_1(t_1, t_2) = \sum_{t=t_1}^{t_2-1} (1 - \gamma_v)^{t-1} \cdot \gamma_v \cdot \Pr[T_e = t_1, T^* = t_2].$$

Meanwhile, we have

$$\begin{aligned} P_2(t_1, t_2) &= \Pr[e \in \mathcal{G}_1, E'_u \cap \mathcal{G}_2 = \emptyset, T_e = t_1, T^* = t_2] \\ &= \sum_{t=t_1}^{\infty} \sum_{t'=1}^{t_2-1} (1 - \gamma_v)^{t+t'-2} \cdot \gamma_v^2 \cdot \Pr[T_e = t_1, T^* = t_2] \\ &= \sum_{t'=1}^{t_2-1} (1 - \gamma_v)^{t_1+t'-2} \cdot \gamma_v \cdot \Pr[T_e = t_1, T^* = t_2] \\ &\geq \sum_{t=t_1}^{t_2-1} (1 - \gamma_v)^{t-1} \cdot \gamma_v \cdot \Pr[T_e = t_1, T^* = t_2] = P_1(t_1, t_2). \end{aligned}$$

Combining all these facts, the proof is complete. \square

Proposition 14. *Consider the instance in Figure 1. For any $R > 0$, there exist b, n_0, β , and γ such that $\frac{\sigma_{\text{IC}}(\{v\})}{\sigma_{\text{SIR}}(\{v\})} > R$.*

Proof. Since the parameters satisfying Equation (1), we can calculate the IC parameter p for the dashed edges as follows

$$p = \sum_{t=1}^{\infty} (1 - \gamma)^{(t-1)} \cdot \gamma \cdot (1 - (1 - \beta)^t) = 1 - \frac{\gamma(1 - \beta)}{\gamma + \beta - \gamma \cdot \beta}, \quad (3)$$

where the last equality follows from standard computations of geometric series.

Notice that, by our definition of solid edges, if at least one of the in-neighbors of u is infected, u will be infected with probability 1, and this is true under both models. Let $p_1(b)$ be the probability that the node u gets infected in IC and $p_2(b)$ be that in SIR. One can easily verify that

$$p_1(b) = 1 - (1 - p)^b = 1 - \left(\frac{\gamma \cdot (1 - \beta)}{\gamma + \beta - \gamma \cdot \beta} \right)^b$$

according to Equation (3), and

$$p_2(b) = 1 - \sum_{t=1}^{\infty} (1-\gamma)^{(t-1)} \cdot \gamma \cdot (1 - (1-\beta)^{b-t}) = \frac{\gamma \cdot (1-\beta)^b}{1 - (1-\gamma) \cdot (1-\beta)^b}.$$

Setting $\gamma = b^{-0.5}$ and $\beta = b^{-1.5}$,

$$\begin{aligned} p_1(b) &= 1 - \left(\frac{b^{-0.5} \cdot (1 - b^{-1.5})}{b^{-0.5} + b^{-1.5} - b^{-2}} \right)^b \\ &\leq 1 - \left(\frac{b^{-0.5}}{b^{-0.5} + 2b^{-1.5}} \right)^b \\ &= 1 - \left(\frac{2b}{1+2b} \right)^b = 1 - \left(1 - \frac{1}{1+2b} \right)^b, \end{aligned}$$

where the second inequality holds when $b^{-1.5} \leq \frac{1}{2}$. Therefore, $p_1(b)$ tends to $1 - e^{-1/2}$ when b goes to infinity. On the other hand,

$$p_2(b) = \frac{b^{-0.5} \cdot (1 - b^{-1.5})^b}{1 - (1 - b^{-0.5}) \cdot (1 - b^{-1.5})^b} = \frac{b^{-0.5} \cdot (1 - b^{-1.5})^b}{1 - (1 - b^{-1.5})^b + b^{-0.5} \cdot (1 - b^{-1.5})^b}.$$

Hence, $p_2(b)$ tends to 0 when b goes to infinity since $b^{-0.5} \cdot (1 - b^{-1.5})^b$ tends to 0.

Finally, under both models, those n_0 vertices on the right-hand side in Figure 1 will be infected with probability 1 if u is infected. Therefore, we have

$$\sigma_{\text{IC}}(v) = \sum_{u' \in V} \Pr[u' \text{ gets influenced by } v] \geq n_0 \cdot p_1(b), \quad (4)$$

and

$$\sigma_{\text{SIR}}(v) = \sum_{u' \in V} \Pr[u' \text{ gets influenced by } v] \leq (b+1) + n_0 \cdot p_2(b). \quad (5)$$

Combining Equation (4) and Equation (5),

$$\frac{\sigma_{\text{SIR}}(v)}{\sigma_{\text{IC}}(v)} \leq \frac{(b+1) + n_0 \cdot p_2(b)}{n_0 \cdot p_1(b)}.$$

Since $p_1(b)$ tends to a positive constant $1 - e^{-1/2}$ and $p_2(b)$ tends to 0 as $b \rightarrow \infty$, the ratio $\frac{\sigma_{\text{SIR}}(v)}{\sigma_{\text{IC}}(v)}$ tends to 0 when $b \ll n_0$ and b goes to infinity (for example, we can set $n_0 = b^2$ and let $b \rightarrow \infty$). \square